Sustainable Cities and Society 62 (2020) 102382

Contents lists available at ScienceDirect

Sustainable Cities and Society

journal homepage: www.elsevier.com/locate/scs

Temporary reduction in fine particulate matter due to 'anthropogenic emissions switch-off' during COVID-19 lockdown in Indian cities

Prashant Kumar*, Sarkawt Hama, Hamid Omidvarborna, Ashish Sharma, Jeetendra Sahani, K.V. Abhijith, Sisay E. Debele, Juan C. Zavala-Reyes, Yendle Barwise, Arvind Tiwari

Global Centre for Clean Air Research (GCARE), Department of Civil and Environmental Engineering, Faculty of Engineering and Physical Sciences, University of Surrey, Guildford GU2 7XH, United Kingdom

ARTICLE INFO

Keywords:
Coronavirus pandemic
SARS-CoV-2 Virus
Air pollution
Health and economic impacts
$PM_{2.5}$ concentration
Emission switch-off

ABSTRACT

The COVID-19 pandemic elicited a global response to limit associated mortality, with social distancing and lockdowns being imposed. In India, human activities were restricted from late March 2020. This 'anthropogenic emissions switch-off' presented an opportunity to investigate impacts of COVID-19 mitigation measures on ambient air quality in five Indian cities (Chennai, Delhi, Hyderabad, Kolkata, and Mumbai), using in-situ measurements from 2015 to 2020. For each year, we isolated, analysed and compared fine particulate matter ($PM_{2.5}$) concentration data from 25 March to 11 May, to elucidate the effects of the lockdown. Like other global cities, we observed substantial reductions in $PM_{2.5}$ concentrations, from 19 to 43% (Chennai), 41–53% (Delhi), 26–54% (Hyderabad), 24–36% (Kolkata), and 10–39% (Mumbai). Generally, cities with larger traffic volumes showed greater reductions. Aerosol loading decreased by 29% (Chennai), 11% (Delhi), 4% (Kolkata), and 1% (Mumbai) against 2019 data. Health and related economic impact assessments indicated 630 prevented premature deaths during lockdown across all five cities, valued at 0.69 billion USD. Improvements in air quality may be considered a temporary lockdown benefit as revitalising the economy could reverse this trend. Regulatory bodies must closely monitor air quality levels, which currently offer a baseline for future mitigation plans.

1. Introduction

COVID-19, the novel coronavirus disease caused by SARS-CoV-2 (severe acute respiratory syndrome coronavirus 2), was first identified in the Hebei district of Wuhan, China, in December 2019. This infectious disease spread rapidly from China to other countries across the world, and the outbreak was declared a global pandemic on 12 March 2020 by the World Health Organization (WHO, 2020a). The ongoing pandemic has disrupted the lives of billions of people and caused more than 278,994 deaths worldwide as of 11 May 2020 (WHO, 2020b). The United States of America (USA), the United Kingdom (UK), and Italy have experienced the greatest impact to date (11 May 2020), with death tolls of around 76,916, 31,855, and 30,560, respectively (WHO, 2020b). Asian countries, such as India, are not spared where the population density is high (Kumar et al., 2013) and the spread of COVID-19 is yet to reach its peak.

The first case of COVID-19 in India was reported on 30 January 2020 in Kerala, a southern state (PIB, 2020). After a preventive social distancing initiative on 22 March 2020 in the form of a 14-h self-quarantine curfew called the *'Janata Curfew'*, the Government of India (GoI) announced a complete lockdown of both internal and external borders, and social isolation measures came into effect on 25 March 2020 for the entire 1.3 billion population to prevent the spread of COVID-19. The lockdown has been renewed four times to date, with the

Abbreviations: AOD, aerosol optical depth; AQI, air quality index; CO, carbon monoxide; CO_2, carbon dioxide; COVID-19, Coronavirus disease 2019; EPA, Environmental Protection Agency; ER, excess risk; ESA, European Space Agency; GEV, generalized extreme value; GoI, Government of India; HB, health burden; MODIS, moderate resolution imaging spectroradiometer; MSL, mean sea level; NASA, National Aeronautics and Space Administration; NH_3, ammonia; NO_2, nitrogen dioxide; O_3, ozone; PDF, probability density function; PM, particulate matter; $PM_{2.5}$, PM with aerodynamic diameter of $\leq$ 2.5 µm; PM_{10}, PM with aerodynamic diameter of $\leq$ 10 µm; RH, relative humidity; RR, relative risk; SARS-CoV-2, Severe Acute Respiratory Syndrome Coronavirus 2; SO_2, sulphur dioxide; SSEC, Space Science and Engineering Centre; TROPOMI, TROPOspheric monitoring instrument; UK, United Kingdom; USA, United States of America; USD, United States Dollar; VSL, value of statistical life; WHO, World Health Organization

* Corresponding author.
E-mail addresses: P.Kumar@surrey.ac.uk, Prashant.Kumar@cantab.net (P. Kumar).

https://doi.org/10.1016/j.scs.2020.102382
Received 31 May 2020; Received in revised form 21 June 2020; Accepted 24 June 2020
Available online 13 July 2020

Table 1
Summary of recent studies on COVID-19 and air quality impacts.

Study area (city, country)	Key findings	Author (year)
India (Delhi, Mumbai, Kolkata and Bangalore)	• Assessed overall impact of social and travel lockdown in five megacities of India and evaluated spatiotemporal variations in five criteria pollutants over two time periods, i.e., March-April 2019 and March-April 2020 and 10th-20th March 2020 (before lockdown) and 25th March to 6th April 2020 (during lockdown). • Statistically significant reduction was found in all megacities for all pollutants except for O_3, with concentration declines in $PM_{2.5}$ (~41%) PM_{10} (52%), NO_2 (51%) and CO (28%) during the lockdown phase in Delhi when compared to before lockdown. Similar reductions were observed for other megacities.	Jain and Sharma (2020)
India (Delhi)	• Analysed PM_{10}, $PM_{2.5}$, SO_2, NO_2, CO, O_3 and NH_3 over 34 monitoring stations in Delhi during pre-lockdown periods and during the lockdown. • Air quality significantly improved during lockdown, with reductions of 60% (PM_{10}), 39% ($PM_{2.5}$), 53% (NO_2) and 30% (CO) compared to 2019.	Mahato et al. (2020)
India (Kolkata)	• Measured atmospheric CO_2 levels with a portable CO_2 analyzer at 12 sites during April 2019 (pre-lockdown) and April 2020 (post-lockdown). • 30–40% decrease in CO_2 levels with significant temporal variation was observed ($p < 0.01$), but no statistically significant variation was observed between sites.	Mitra et al. (2020)
India (22 cities in different regions)	• Examined impact of lockdown measures on criteria pollutant (PM_{10}, $PM_{2.5}$, CO, NO_2, O_3 and SO_2) concentration reductions and analysed data between 16 March to 14 April from 2017 to 2020. • Compared to previous years (2017 – 2019), during lockdown periods, reductions in concentrations were up to 43% ($PM_{2.5}$), 31% (PM_{10}), ~52% (mean excessive PM risks), 10% (CO), and 18% (NO_2), while an increase of 17% in O_3 and negligible changes in SO_2 were detected. Reductions in AQI were up to 44% (North), 33% (South), 29% (East), 15% (Central) and 32% (West) India.	Sharma et al. (2020)
India	• Based on data-driven estimation methods and curve fitting, a 30-day projection of the effectiveness of preventive measures (social isolation and lockdown) on the spread of COVID-19 in India was developed. • Authors highlighted that the proposed method well estimated and predicted the positive cases and number of recovered cases within a certain range and will be a beneficial tool for policymakers and health officials.	Tomar and Gupta (2020)
Brazil (São Paulo)	• Assessed impacts of partial lockdown in São Paulo on concentration levels of CO, NO, NO_2, and O_3. • CO, NO, NO_2, and O_3 concentrations reduced by 65, 77, 54 and 30%, respectively, during the lockdown period.	Nakada and Urban (2020)
China	• Data from the TROPOspheric Monitoring Instrument (TROPOMI) sensor on-board ESA's Sentinel-5 satellite showed reductions in NO_2 concentrations due to lockdown near Wuhan, China (~30%) and worldwide. • CO_2 also decreased by 25% in China and by 6% worldwide. Fatalities might have decreased due to reduced air pollution levels.	Dutheil, Baker, and Navel (2020)
China	• Daily mortality due to air pollution and COVID-19 between Dec 2019 and Mar 11th 2020 showed huge differences, indicating that lockdown likely saved more lives by preventing ambient air pollution than by preventing infection. • NASA satellite images showed reductions of up to 30% in NO_2 levels and about 25% carbon emissions (≈100 Mt equivalent to 6% of the global emissions) over the same period in Feb 2020 due to quarantine.	Isaifan (2020)
China (330 cities) and USA (New York)	• Evaluated the significance of environmental (including air quality) impacts of the COVID-19 lockdown in 330 Chinese cities and NewYork (USA). • When compared with 2019 data, air quality in 2020 improved by 11% across 330 cities of China and 50% in New York (USA).	Saadat, Rawtani, and Hussain (2020)
China	• Investigated impact of reduced anthropogenic activities due to lockdown on air pollution using simulation with the community multi-scale air quality model between 01 Jan and 12 Feb 2020 and compared three air pollution scenarios. • Decreased $PM_{2.5}$ in Beijing, Shanghai, Guangzhou, and Wuhan by 9.23, 6.37, 5.35, and 30.79μgm^{-3}, respectively. However, reduction ratios of $PM_{2.5}$ concentrations were smaller than those of precursor emissions, partially due to unfavorable meteorological conditions.	Wang, Chen, Zhu, Wang, and Zhang (2020)
China	• Assessed the dynamic environmental (including air quality) impacts of COVID-19 in China during the period of Jan-Mar 2020 compared to 2019. • Reduction in CO_2 emissions by > 25% ~ 1M tonne of C or 6% of global emissions over two weeks (spring festival 2020 and 2019). Satellite data: decline in NO_2 (> 30% China; 50% Wuhan). Air-pollutant monitoring in 337major cities (Jan-Mar 2020): Decline in $PM_{2.5}$ (14.8%), NO_2 (25%), CO (6.2%), PM_{10} (20.5%), SO_2 (21.4%); no change in O_3. • Reduced economic activities decrease energy consumption and hence environmental pollution.	Wang and Su (2020)
China and Europe (France, Germany, Spain, and Italy)	• Studied positive and negative impacts of the COVID-19 lockdown on the environment in severely affected countries such as China, USA, Italy and Spain. • Quarantine led to reduced air pollutant concentrations in: (i) China, for NO_2 (12.9–22.8μgm^{-3}, Wuhan) and $PM_{2.5}$ (18.9μgm^{-3} in 367 cities (Wuhan-1.4μgm^{-3})) ~ 20 – 30% between the monthly average for February 2020 against monthly averages for last three years (February 2017 – 2019); and (ii) Europe (Rome, Madrid, and Paris), in NO_2 and $PM_{2.5}$ concentrations in February 2020 compared to previous three years (2017 – 2019).	Zambrano-Monserrate, Ruano, and Sanchez-Alcalde (2020)

(*continued on next page*)

Table 1 (*continued*)

Study area (city, country)	Key findings	Author (year)
China (120 cities)	● Using generalised additive models, the authors explored relationships between ambient air pollutant ($PM_{2.5}$, PM_{10}, SO_2, CO, NO_2 and O_3) concentrations and COVID-19 infection, utilising associations between meteorological variables (temperature, wind speed, RH) and daily COVID-19 confirmed cases. ● Significant positive correlations were found between pollutant concentrations ($PM_{2.5}$, PM_{10}, NO_2 and O_3) and newly COVID-19 confirmed cases. For example, a 10μgm^{-3} increase in $PM_{2.5}$, PM_{10}, NO_2, and O_3 was linked to a 2.24%, 1.76%, 6.94%, and 4.76% increase in daily counts of confirmed cases, respectively. Conversely, a 10 μg m^{-3} increase in SO_2 was linked to a 7.79% decrease in COVID-19 confirmed cases.	Zhu et al. (2020)
New York, Los Angeles, Zaragoza, Rome, Dubai, Delhi, Mumbai, Beijing and Shanghai	● Dec 2019-Mar 2020 (COVID-19 outbreak period) compared with 2017 – 2019 for changes in $PM_{2.5}$ concentration (data from USEPA). ● Decline in $PM_{2.5}$ concentration in March 2020 compared to March 2019in. Dubai (11%), Rome (no change), Delhi (35%), Mumbai (14%), Beijing (50%), Shanghai (50%), New York (32%), Los Angeles (4%). No change in Zaragoza.	Chauhan and Singh (2020)
China, Spain, France, Italy, USA	● Study compiled environmental data released by NASA and ESA (European Space Agency) before and after the pandemic (Jan-Mar, 2019 and 2020) and discussed its impact on environmental quality. ● Found reductions in NO_2 levels of up to 20 – 30% in Wuhan (China), Spain, France, Italy and the USA.	Muhammad, Long, and Salman (2020)
Global	● Studied the impact of weather variables and air pollution (CO_2, NO_2, PM) on the global infection and spreading rate of COVID-19. ● Air pollution was linked to an increased risk of COVID-19 infection and, therefore, strict and early lockdown measures (particularly in India and China) led to significant reductions in concentrations of NO_2 and CO_2 and this was observed across many metropolitan cities globally.	Paital (2020)
Global (27 countries, China, India and Europe)	● Using satellite data and a network of more than 10,000 air quality stations, the authors investigated whether or not reduced air pollution levels during Feb-Mar 2020 were related to COVID-19 lockdown events. ● 7400 (340 to 14,600) premature deaths and 6600 (4900 to 7900) pediatric asthma cases were avoided over two weeks post-lockdown. $PM_{2.5}$-related avoided premature mortality was estimated for China as 1400 (1100 to 1700) and for India as 5300 (1000 to 11,700). Globally, 0.78 (0.09–1.5) million premature deaths and 1.6 (0.8–2) million pediatric asthma cases could be avoided in 2020, assuming the lockdown-induced reduction in concentrations is maintained throughout the year.	Venter et al. (2020)
Iran (Tehran, Mazandaran, Alborz, Gilan, and Qom)	● Examined the influence of several parameters on COVID-19 spread. Parameters included weather variables (e.g. average temperature, average precipitation, humidity, wind speed, and average solar radiation), number of COVID-19 infected people, population density, intra-provincial movement, and infection days. ● Population density and intra-provincial movement showed a direct correlation with the infection outbreak, while regions with comparatively low wind speed, humidity and solar radiation exposure showed higher rates of infection due to favourable conditions for virus survival.	Ahmadi, Sharifi, Dorosti, Ghoushchi, and Ghanbari (2020)
Iran	● Air samples from 2 – 5 m of patients' beds were collected to measure airborne transmission of COVID-19. ● All tests results were negative, with no positive readings within 2m distance of patients.	Faridi et al. (2020)
Italy (Brescia, Lodi, Monza, Alessandria, Milan, Turin, Padua, Bergamo and Cremona, Rovigo and Genoa, Lombardy region)	● Determined associations between infected people and environmental, demographic and geographical factors governing transmission dynamics of COVID-19. ● Cities with more than 100 days of air pollution (i.e. surpassing PM_{10} or O_3 limits) showed significantly higher average numbers of infected individuals (~3600 infected individuals on 7 April 2020) than in cities with less than 100 days of air pollution (~1000 infected individuals).	Coccia (2020)
Spain (National)	● Using generalised linear mixed models, the authors estimated the shape of the epidemic curve of accumulated cases and evaluated the effect of the intervention introduced by the Spanish government to mitigate the COVID-19 epidemic. ● After one day of implementation of the measures, the variation rate of accumulated cases was reported to reduce daily on average from 3.1–5.1%. However, until 14 March 2020, the introduced measures to reduce the epidemic curve of COVID-19 have not reached the planned phase.	Saez, Tobias, Varga, and Barceló (2020)
Spain (Barcelona)	● Investigated changes in air pollution levels during the lockdown in terms of urban background and traffic air quality observed stations. ● After two weeks of lockdown, the authors found a substantial reduction in BC (-45%) and NO_2 (-51%), mostly related to traffic emissions. PM_{10} also decreased from -28 to -31%, whereas levels of O_3 increased from +33 to +57%.	Tobías et al. (2020)
Turkey (Nine cities : Istanbul, Izmir, Ankara, Konya, Kocaeli, Sakarya, Isparta, Bursa and Adana, Turkey)	● Studied the impact of meteorological variables (temperature, dew point temperature, humidity, and wind speed) on the COVID-19 pandemic over four periods (1, 3, 7, and 14 days).	Şahin (2020)

(*continued on next page*)

Table 1 (*continued*)

Study area (city, country)	Key findings	Author (year)
	• Population, wind speed 14 days ago, and temperature on the day showed the highest correlations, respectively.	
USA (New York)	• Investigated correlations between climate indicators (average temperature, minimum temperature, maximum temperature, rainfall, average humidity, wind speed, and air quality) and the COVID-19 pandemic. • Meteorological variables (average temperature, minimum temperature) and air quality showed strong correlation with the COVID-19 pandemic.	Bashir, Ma et al. (2020)
USA (Nationwide)	• Investigated associations between long-term average exposure to $PM_{2.5}$ and increased risk of COVID-19 death in the United States. • Found that an increase of 1 μg m^{-3} in $PM_{2.5}$ is associated with an 8% increase in the COVID-19 death rate (95% CI 2%–15%).	Wu, Nethery et al. (2020)
Malaysia and Southeast Asia	• Investigated air quality impact of lockdown. Decrease in AOD (Singapore, Brunei, Malaysia and the Philippines), tropospheric NO_2 column density (27 − 34% in most countries except for Ho Chi Minh and Yangon cities) was noted. AODs remained very high (up to 2) in northern Southeast Asia due to extensive forest fires and agricultural burning. • In Malaysia (March-April 2020), decrease in AOD (urban area: 40 − 70%), PM_{10} (industrial: 28–39%, urban: 26 − 31%), $PM_{2.5}$ (industrial: 20–42%, urban: 23 − 32%), NO_2 (industrial: 33–46%, urban: 63 − 64%), SO_2 (urban: 9 − 20%), and CO (urban: 25 − 31%) compared with 2018 and 2019 was noted.	Kanniah, Zaman, Kaskaoutis, and Latif (2020)
Southern European cities (Nice, Rome, Valencia and Turin) and Wuhan (China)	• Presented the challenge of reducing the formation of secondary pollutants such as O_3 even with lockdown's reduced emission. In comparison to 2017 − 19, O_3 increased (24% in Nice, 14% in Rome, 27% in Turin, 2.4% in Valencia and 36% in Wuhan) due to reduced NOx and lower O_3 titration by NO, while reductions were observed in NO_2 (∼53% in Europe and 57% in Wuhan), NO (∼63% in Europe), and $PM_{2.5}$ and PM_{10} (∼8% in Europe and ∼42% in Wuhan) at urban stations. NO_2 and NO decreased by ∼65% and ∼78% respectively at traffic stations in Europe. • Last years' weekend comparison showed that NOx was ∼ 49% lower in all cities, O_3 was ∼10% higher in Southern Europe and 38% higher in Wuhan, PM was similar (∼6%) in Southern Europe.	Sicard et al. (2020)
Yangtze River Delta Region (China)	• The WRF-CAMx modelling system and monitoring data were applied to investigate the impact of lockdown on air quality and sources of residual pollution for future air pollution control. • Reductions in SO_2 (16–26%), NOx (29–47%), $PM_{2.5}$ (27–46%) and VOCs (37–57%) emissions were observed. Declines in $PM_{2.5}$ (31.8%, 33.2%), NO_2 (45.1%, 27.2%) and SO_2 (20.4%, 7.6%) were observed during the two periods of lockdown compared to 2019, however ozone increased greatly. Though primary emissions reduced (15%–61%), $PM_{2.5}$ varied little (15 − 79μgm^{-3}), suggesting high background and residual pollution. • Source apportionment pointed to industry (32.2–61.1%), mobile (3.9–8.1%), dust (2.6–7.7%), and residential (2.1–28.5%) sources of $PM_{2.5}$ and a 14.0–28.6% contribution of long-range transport from northern China.	Li, Li et al. (2020)
44 cities in northern China	• Estimated the effects of COVID-19 related travel restrictions on air pollution. • The AQI decreased by 7.80%, and SO_2, $PM_{2.5}$, PM_{10}, NO_2, and CO decreased by 6.76%, 5.93%, 13.66%, 24.67%, and 4.58% respectively. Human movements were reduced by 69.85%, partially causing reduction in the AQI, $PM_{2.5}$, and CO, while completely mediating SO_2, PM_{10}, and NO_2 reductions.	Bao and Zhang (2020)
Almaty (Kazakhstan)	• Analysed the effects of COVID-19 lockdown on air pollutants. Reductions in $PM_{2.5}$ (21%, spatial variations: 6–34%), CO (49%) and NO_2 (35%) were observed compared to 2018–2019, whereas O_3 increased by 15% compared to 17 days before the lockdown. Benzene and toluene were 2–3 times higher than for 2015–2019. • Pointed towards non-traffic-related sources, such as coal-fired combined heat and power plants, household heating systems, garbage burning and bathhouses.	Kerimray et al. (2020)
Delhi (India)	• Assessed pollutant datasets and observed a significant improvement in ambient air quality due to lockdown. • NOx reduced by ∼14 times the peak value (342 to 24ppb from 12 January to 30 March 2020). Significant reduction in the PM_{10}, $PM_{2.5}$, NH_3, SO_2, NO, NO_2, NOx and CO concentrations.	Kotnala, Mandal, Sharma, and Kotnala (2020)
Review (Global)	• Reviewed the evidence for SARS-CoV-2 transmission by particulate matter pollutants. • $PM_{2.5}$ was suggested to transmit coronavirus via aerosols in Italy and Wuhan. $PM_{2.5}$ may have direct correlation with virus transmission and related mortality.	Sharma and Balyan (2020)
Lucknow and New Delhi (India)	• Analysed primary air pollutant data before and after lockdown (21-days). Significant decline in $PM_{2.5}$, NO_2 and CO was seen in both cities, with less significant decline in SO_2.	Srivastava, Kumar, Bauddh, Gautam, and Kumar (2020)

(continued on next page)

Table 1 (*continued*)

Study area (city, country)	Key findings	Author (year)
	• Perceptible air pollution mitigation was due to adoption short and periodic lockdowns.	
Northern China	• Quantified surface $PM_{2.5}$, NO_2, CO, and SO_2 reductions during the lockdown. • $PM_{2.5}$ and NO_2 decreased by 29 ± 22% and 53 ± 10%, respectively, but O_3 increased by a factor 2.0 ± 0.7. Similar reductions ($PM_{2.5}$: 31 ± 6%, NO_2: 54 ± 7%) and increase (O_3: 2.2 ± 0.2 fold) were noted in the urban area of Wuhan.	Shi and Brasseur (2020)
Rio de Janeiro (Brazil)	• Discussed the partial lockdown impact on city air quality, comparing 2019 and weeks prior to the virus outbreak. • CO, related to light-duty vehicular emissions, reduced to 30.3–48.5%. Due to industrial and diesel input, NO_2 decreased to a lower extent and PM_{10} reduced only during the first week. O_3 increased due to the decrease in nitrogen oxide levels in a VOC-controlled scenario. • In April, vehicular flux and people movement increased due to public disregard of lockdown. Compared to 2019, NO_2 and CO median values were 24.1–32.9 and 37.0–43.6% lower. Meteorological interferences (e.g. transport of industrial pollutants) might have also impacted the results.	Dantas, Siciliano, França, da Silva, and Arbilla (2020)
Global	• Tested the hypothesis of improved environmental quality due to lockdown induced atmospheric pollutants reduction. • COVID-19 cases in the tropical regions were relatively lower than the European and American regions. Reductions in NO_2 (Substantial: 0.00002mol m^{-2}), CO (low: < 0.03mol m^{-2}) and AOD (low-to-moderate: ~0.1–0.2) were observed in the major hotspots of COVID-19 outbreak during Feb–Mar 2020. High hazard was projected in major areas of the globe (absolute humidity: $4-9$g m^{-3}) during Apr–Jul 2020. The northern hemisphere may be more susceptible in May–Jul 2020 while tropical regions in Oct–Nov 2020. • Scope for restoring the global environment from the ill-effects of anthropogenic activities through temporary shutdown measures was suggested.	Lal et al. (2020)
California (USA)	• Employed Spearman and Kendall correlation tests to analyse the association of $PM_{2.5}$, PM_{10}, SO_2, NO_2, Pb, VOC, and CO with COVID-19 cases. • PM_{10}, $PM_{2.5}$, SO_2, NO_2, and CO had significant correlation with the COVID-19 epidemic and adoption of green environmental policies was promoted to shield human life.	Bashir, Bilal, and Komal (2020)
Northern China	• Evaluated AQI, $PM_{2.5}$, PM_{10}, CO, SO_2, NO_2, and O_3 changes during the COVID-19 control period. The AQI decreased from 89.6–71.6. 322 out of 366 cities experienced AQI decline. All pollutants decreased except O_3 because of less scavenging of HO_2 due to lower fine particle loadings. Reductions in NO_2, $PM_{2.5}$, CO, and SO_2 were linked to reduced activities of transportation, secondary industries and industrial sector respectively. • Importance of reactions between gaseous and particulate pollutants, and control of residential emissions were illustrated. Lowering both NOx and VOCs will be needed to control O_3.	Wang, Yuan et al. (2020)
Milan (Italy)	• Assessed the effect of partial and total lockdown on air quality in meteorologically comparable periods. • A significant reduction of PM_{10}, $PM_{2.5}$, BC, benzene, CO and NOx was observed mainly due to reduced vehicular traffic. SO_2 also dropped but remained unchanged in the adjacent areas. O_3 increased due to the minor NO concentration and was more accentuated in the adjacent areas with reduced concentrations of benzene.	Collivignarelli et al. (2020)
Salé City (Morocco)	• Analysed air pollutants before and during the lockdown period. PM_{10}, SO_2 and NO_2 concentrations were reduced respectively by 75%, 49% and 96%. • The three-dimensional air mass backward trajectories, using the HYSPLIT model, demonstrated that long-range transported aerosol contributions out-balanced the reductions in locally emitted PM_{10}. Differences in the air mass back trajectories and the meteorology between these two periods were shown.	Otmani et al. (2020)
Dwarka river basin within Jharkhand and West Bengal (India)	• Explored the impact of forced lockdown on PM_{10}, land surface temperature, river water quality and noise using image- and field-derived data. • PM_{10} concentration reduced from $189-278$μgm^{-3} in the pre-lockdown period to $50-60$μgm^{-3} after 18 days of lockdown in selected four stone crushing clusters.	Mandal and Pal (2020)

first, second, third, and fourth phases ending on 14 April, 03 May, 17 May, and 31 May 2020, respectively (see details in Section 2.2). As of 11 May 2020, the total number of cases reported in India stands at 67,152, with 40,917 recoveries and 2206 deaths (COVID-19.in, 2020).

Similar COVID-19 lockdowns throughout the world have entailed self-isolation, reduced personal travel and outdoor activities, and business closures across all sectors, including: commercial; industrial; construction; transport - both road and air; academic; retail; and social, such as restaurants, theatres, cinemas and sports stadiums. Global action to mitigate the pandemic has consequently involved switching off most pollutant emission sources. Therefore, we refer to the COVID-19 outbreak here as an 'anthropogenic emissions switch-off' experiment that indicates a pollution baseline, which cities may aim to achieve under 'normal' conditions. This switch-off offers important educational opportunities regarding potential control systems and regulations for improved urban air quality in the future. Besides a few exceptional pollution episodes, such as increased levels of fine particulate matter ($PM_{2.5}$, with aerodynamic diameter $\leq 2.5\,\mu m$) in the central United States in March due to long-range transport of particles from agricultural burning in Mexico (Schiermeier, 2020), many cities worldwide have seen blue skies for the first time in several decades. This is illustrated by Table 1, which shows appreciable gaseous and PM concentration reductions of up to 77% (in NO; São Paulo, Brazil) and 60% (in PM_{10}; Delhi, India) across cities worldwide during lockdown periods.

Beyond coming into contact with an infected person's coughing/sneezing or touching contaminated surfaces (Kumar & Morawska, 2019), poor indoor ventilation has also been linked to COVID-19 spread (Brittain et al., 2020; Morawska & Cao, 2020) and outdoor aerosols containing viral RNA (Setti et al., 2020). For example, Li, Qian et al. (2020) reported the prolific spread of COVID-19 in a poorly ventilated restaurant in Wuhan, China. In another study, Liu et al. (2020) examined the potential for aerosol-assisted transmission of the virus by measuring viral RNA in different places inside two Wuhan hospitals in February and March 2020. They reported a high concentration of viral RNA that matched peaks in both sub- and super-micrometre particle ranges and highlighted the potential transmission of SARS-CoV-2 via aerosols. Similarly, Setti et al. (2020) reported the RNA of COVID-19 in aerosol particles in Italy. However, it is not yet known whether or not this coronavirus interacts with airborne aerosol particles and much needs to be understood in this respect. The individual impact of COVID-19 is greatest for those with weak immune systems, such as the elderly, and those with pre-existing health conditions. For example, Wu, Leung et al. (2020) reported that a COVID-19 infected person > 59 years of age has a 5.1-times higher risk of dying, compared with only 0.6-times for those < 39 years old. The analogy that air pollution is linked with respiratory and cardiovascular disease (Heal, Kumar, & Harrison, 2012) and that cities with high air pollution may therefore expect to experience a more prominent impact of COVID-19 is hypothesised. Early evidence supports this hypothesis, albeit based on several assumptions. For example, Zhu et al. (2020) applied generalised additive models and reported a 2.24% increase in COVID-19 confirmed cases for each $10\,\mu g\,m^{-3}$ increase in $PM_{2.5}$ concentrations across Chinese cities. Likewise, a nationwide cross-sectional study in the US associated an increase of $1\,\mu g\ m^{-3}$ in $PM_{2.5}$ concentration with an 8% increase in COVID-19 death rates (Wu, Nethery, Sabath, Braun, & Dominici, 2020). While links to reduced air pollution during lockdown with human health impacts can be understood, linking COVID-19 with air pollution and death rates together remains a grey area that will require detailed scientific assessments to develop a consensus.

India faces air pollution challenges due to its explosive population growth and rapid expansion of industrial development in recent decades. As a result of economic growth, air pollutant concentrations have reached alarming levels that consistently exceed ambient air quality standards. This has exacerbated human health risks and increased premature mortality in surrounding communities (Guo et al., 2017; Mukherjee & Agrawal, 2018; Sharma, Zhang, Gao, Zhang, & Kota, 2020; Shukla, Kumar, Mann, & Khare, 2020). For example, 77% of the Indian population in 2017 were exposed to annual mean ambient $PM_{2.5}$ concentrations of more than $40\,\mu g\ m^{-3}$ (ICMR-PHFI-IHME, 2017). $PM_{2.5}$ is predominantly generated from vehicle combustion engines, residential/industrial fuel burning and secondary aerosol formation (Guo et al., 2017; Guo, Kota, Sahu, & Zhang, 2019; Hama et al., 2020; Kumar, Gulia, Harrison, & Khare, 2017). In India, studies on air quality changes associated with COVID-19 are limited but clearly show an appreciable reduction in criteria air pollutants (e.g. PM_{10}, $PM_{2.5}$, CO, NO_2, O_3, SO_2, and NH_3), mainly due to decreased on-road vehicles and closure of non-essential industries (Mahato, Pal, & Ghosh, 2020; Sharma et al., 2020). For example, Sharma et al. (2020) used a WRF-AERMOD modeling system to demonstrate an overall decline of 43% in $PM_{2.5}$ during the lockdown of March 2020, when compared with similar months in previous years. Similarly, Mahato et al. (2020) reported a reduction of more than 50% in $PM_{2.5}$ and PM_{10} concentrations, and Venter, Aunan, Chowdhury, and Lelieveld (2020) linked the first two weeks of lockdown in India to a reduction in $PM_{2.5}$ related premature mortality of roughly 5300 (Venter et al., 2020). Chennai, Delhi, Hyderabad, Kolkata, and Mumbai are among the most populated (Table S1) and industrialised Indian cities, where ambient concentrations of $PM_{2.5}$ are ordinarily above WHO annual guideline values of $10\,\mu g\ m^{-3}$ (WHO, 2016). We have targeted these sprawling Indian cities to understand relative changes in $PM_{2.5}$ concentrations due to the impact of lockdown on emission sources before and during the lockdown.

It may be expected that lockdowns to contain the spread of COVID-19 will generally result in reduced urban anthropogenic emission activities, and one can reasonably expect a reduction in concentrations of primary pollutants during lockdown when compared with periods of business as usual. However, what remained unknown was: how much reduction lockdown led to, in quantitative terms; whether this reduction occurred to a similar degree in all cities; and what additional factors may influence any differences between cities. As illustrated by Table 1, COVID-19 related air quality studies for Indian cities are limited. Such studies have typically covered varying days of the early lockdown period and involved analyses based on publicly available data from monitoring stations (e.g. Mahato et al., 2020; Sharma et al., 2020) and/or modelling exercises (e.g. Mitra et al., 2020). Therefore, varied estimations of $PM_{2.5}$ concentration reductions have been produced for the same cities, such as 35–39% for Delhi (Chauhan & Singh, 2020; Mahato et al., 2020), 30–40% for Kolkata (Mitra et al., 2020), and 14–43% for Mumbai (Chauhan & Singh, 2020; Sharma et al., 2020). We cover the extended duration of lockdown in five Indian cities (Chennai, Delhi, Hyderabad, Kolkata, and Mumbai) and go beyond the scope of previous studies by evaluating the impact of the COVID-19 pandemic's 'anthropogenic emission switch-off', with an aim to: (i) investigate variations and characteristics of $PM_{2.5}$ concentrations during the lockdown in five Indian cities compared to similar periods in the previous five years; (ii) contextualise our own results from Indian cities with others from across the world; (iii) explore potential factors that influence differences between divergent concentration changes in different cities; (iv) monitor the distribution of $PM_{2.5}$ concentrations using theoretical probability density function (PDF) at six different time spans in five Indian cities; (v) reveal a holistic picture of aerosol loadings for each of these cities by utilising aerosol optical depth (AOD) analysis via satellite imagery; and (vi) generate valuations of health and economic impact due to decreased $PM_{2.5}$ concentrations.

2. Materials and methods

2.1. Study areas

Fig. 1 presents the topography of the studied Indian cities (Chennai, Delhi, Hyderabad, Kolkata, and Mumbai). Corresponding tables summarise each city's location, population, population density and traffic

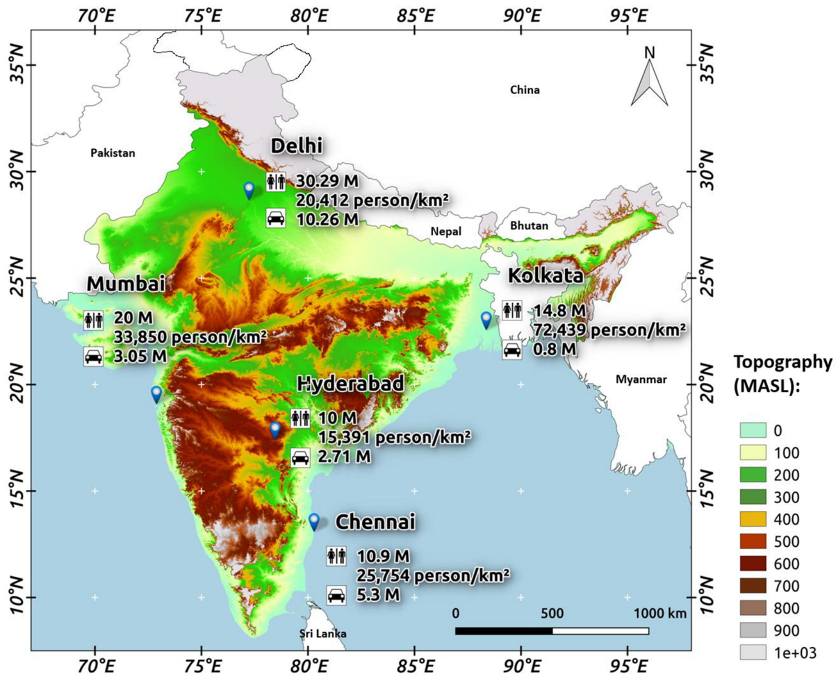

Fig. 1. Topographic map of India, showing the locations, population density and vehicle population in Chennai, Delhi, Hyderabad, Kolkata and Mumbai. References for the data used in this figure, including human and vehicle population data, are available in Table S1.

density (Table S1), known sources and traffic contributions to $PM_{2.5}$ (Table S2), and key features and meteorological characteristics (Table S3). All five cities experience the summer season during the lockdown period of March-May (Table S4). Differences in meteorological conditions between this period of 2020 and of previous years were modest (Table S4), as discussed below.

- **Chennai** is the capital city of the south Indian state of Tamil Nadu, with a population of ~10.9 million and an overall population density of 25,754 per square kilometre (Table S1). The average elevation of Chennai above the mean sea level (MSL) is ~15.8 m (Table S3). The city had about 5.3 million vehicles on its roads in 2017 (Table S1). The dominant wind direction, observed from Chennai airport (12°58′56″N 80°9′49″E), is towards the south (21%), followed by the west (16%) and the east (15%) (Table S3). Pollutants from industrial suburbs in North Chennai (Padi, Avadi and Ambattur) are transported by the wind towards the central and southern parts of the city. The average wind speed, ambient temperature and relative humidity (RH) during the lockdown period in 2020 were 3.0 ± 1.7 m s^{-1}, 30.6 ± 2.8 °C and 71.7 ± 12.8%, respectively.
- **Delhi** is the capital of India and one of the largest megacities of Asia, with an overall population of 30.29 million and a population density of 20,412 per square kilometre (Table S1), as well as the highest number of registered on-road vehicles of all Indian cities (~10.26 million in 2017; Table S1). Delhi has an average elevation of ~216 m. The dominant wind direction, observed at Safdarjung airport (28°35.00′ N, 77°12.48′ E), which is located 3.75 km from the geographical centre of Delhi (India gate), is westerly (nearly 34% of the observed duration during the study period; Table S3). The wind speed, ambient temperature and RH during the lockdown period were 2.5 ± 1.7 m s^{-1}, 31.2 ± 3.1 °C and 43.4 ± 8.6%, respectively.
- **Hyderabad** is the capital city of the south Indian state of Telangana, situated at an altitude of 545 m above MSL (Table S3), with a population of ~10 million and an overall population density of 15,391 per square kilometre (Table S1). The rate of urbanization and infrastructural development in the city has increased over the past decade to about 2.71 million vehicles on the roads of Hyderabad in 2017 (Table S1). Dominant wind direction, recorded (during 2000–2019; Table S3) at Rajiv Gandhi Hyderabad International Airport in Hyderabad (17°14.43′ N, 78°25.73′ E), is towards the west (30%). The wind speed, ambient temperature and RH during the lockdown period were 1.1 ± 0.2 m s^{-1}, 30.5 ± 4.1 °C and 54.9 ± 18.1%, respectively.
- **Kolkata** is the capital city of the East Indian state of West Bengal, and is considered one of the most polluted cities in the world (Scroll, 2019). Kolkata has a population of 14.8 million with an overall population density of 72,439 per square kilometre (Table S1). At just 6.10 m above MSL (Table S3), Kolkata is located in the Ganges Delta of north-eastern India, near the Bay of Bengal and ~80 km west of the border with Bangladesh. This dense city had about 0.8 million vehicles on the roads in 2017 (Table S1). Observed meteorological data (2000–2019) from Netaji Subhas Chandra Bose International Airport (22°39.24′ N, 88°26.80′ E), known as Dum Dum airport (located ~17 km from Kolkata city centre), showed that wind direction is primarily towards the south (34% of the time). The wind speed, ambient temperature and RH during the lockdown period were 1.0 ± 0.6 m s^{-1}, 29.3 ± 3.6 °C and 69.1 ± 17.7%, respectively.
- **Mumbai** is the sixth-largest metropolitan region in the world (Pacione, 2006) and the financial capital of India. It has a population of 20 million at a density of 33,850 per square kilometre (Table S1). With an average elevation of ~12.20 m above MSL (Table S3), the dominant wind direction measured at Chatrapati Shivaji Maharaj airport (Terminal-1; 19°5.50′ N, 72°51.97′ E) is towards the west (36% of the observed duration; Table S3), which highlights the role of meteorological factors in transporting pollutants from the eastern manufacturing districts into the city. Ambient air quality in Mumbai is also significantly affected by vehicle traffic (about 3.05 million on-road vehicles in 2017; Table S1). The wind speed, ambient temperature and RH during the lockdown period in 2020 were 0.8 ± 0.5 m s^{-1}, 29.5 ± 1.8 °C and 81.4 ± 8.6%, respectively.

2.2. Data source

Hourly $PM_{2.5}$ data for Chennai, Delhi, Hyderabad, Kolkata and Mumbai were extracted for the period between January 2015 and May 2020 (Section 2.3). These data are measured using beta-attenuation monitors that are calibrated and maintained as per the protocols of the US EPA (EPA, 2009). The beta-attenuation monitoring method for continuous $PM_{2.5}$ monitoring is used for over 80% of state- and local-level observations in the US (EPA, 2015). The data are available online (https://www.airnow.gov/) and have been used previously by numerous studies in India (e.g. Chen et al., 2020; Wang & Chen, 2019) and elsewhere (e.g. Berman & Ebisu, 2020; Dhammapala, 2019; Martini, Hasenkopf, & Roberts, 2015). As a quality assurance exercise, we followed two approaches: (i) outlier detection and gap-filling techniques to clean the obtained dataset, similar to what Jesus et al. (2020) applied for $PM_{2.5}$ long-term time series, using the forecast package (Hyndman et al., 2019); and (ii) a simpler approach that included removal of all zero, negative and invalid data points after manual inspection of the dataset. The percentage of maximum difference, using both approaches, between $PM_{2.5}$ mean concentrations for all cities during the lockdown in the year 2020, was found to be less than 1%. This low difference was expected since the percentage of total missing data points (i.e. the sum of zero, negative and invalid) during the assessment period was also less than 1%. Most of the gap-filling methods are usually recommended when missing data percentages are greater than 5% (Ottosen & Kumar, 2019; Junger & De Leon, 2015; Junninen, Niska, Tuppurainen, Ruuskanen, & Kolehmainen, 2004). Since these differences in concentrations and the percentage of missing data were modest, we adopted the simpler approach to preserve the site-specific measured data points as-is for further analysis. The cleaned dataset was run through the R statistical package (R Core Team, 2020) in the Open-air software package version 2.6–5 (Carslaw & Ropkins, 2012; Carslaw, 2015) to identify missing periods and assess basic statistics, and to plot the data at each site for further analysis and interpretation.

2.3. Data analyses

The lockdown period in Indian cities (25 March 2020 onwards) is divided into different phases as discussed below. Detailed specifications regarding each phase are presented in the introduction of Section S1. On 22 March 2020 (0700 – 2100 h IST), a 14 -h voluntary public curfew/restraint was imposed as a pre-emptive measure against COVID-19 spread, as suggested by the government. From 25 March 2020 onwards, an official quarantine plan was imposed by the GoI in four phases. *Phase I* (ended 14 April 2020) involved a suspension of nearly all services for 21 days, including transportation and factories but excluding emergency services. *Phase II* (15 April 2020 to 03 May 2020) was an extension of Phase I for an additional 19 days, with a conditional relaxation for certain businesses. A lockdown area classification system (Red/Orange/Green) was initiated during this phase on 16 April 2020. *Phase III* (04 May 2020 to 17 May 2020) remained in place for the subsequent 24 days. Area classification was periodically revised during this phase. *Phase IV* (18 May 2020 to 31 May 2020), a 14-day quarantine, was the most recently updated rule by GoI before submitting this study. The duration between the official initiation of the lockdown restrictions (25 March 2020) and the time we extracted the datasets (11 May 2020) is henceforth referred to as 'lockdown' and was compared with similar periods of the past five years (2015–2019).

2.3.1. Generalized extreme value distribution

The probabilistic distribution of $PM_{2.5}$ exposure concentration during the lockdown period was explored for each city. Estimation of the PDF of $PM_{2.5}$ concentrations before and during lockdown periods was carried out using a generalized extreme value (GEV) model, which is a common statistical approach used in extreme value analysis of air pollution data (Martins et al., 2017). The probability distributions or density function in the GEV distribution model is described by Eq. (1):

$$f_Y(y;\mu,\sigma,k) = exp\left\{-\left[1+k\left(\frac{y-\mu}{\sigma}\right)\right]^{\frac{-1}{k}}\right\} \quad (1)$$

The theoretical density of $PM_{2.5}$ is also estimated using Eq. (1). The variable y is the hourly $PM_{2.5}$ concentration and the parameters μ, σ, and k represent the distribution location, scale, and shape, respectively. The location determines the position of the distribution, the scale determines the size of deviations around the location parameter, and the shape determines the behaviour of the upper tail of the distribution (Coles, 2001). When $k = 0$, Eq. (1) is Gumbel distribution (light tail), when k is positive, Eq. (1) is Frechet distribution (heavy tail) and when k is negative, Eq. (1) is Weibull distribution (upper bounded tail). The estimated shape of $PM_{2.5}$ for each city before and during lockdown is reported in Table S5. The GEV model is fitted to the $PM_{2.5}$ dataset by maximizing the logarithmic likelihood function using the maximum likelihood method (Coles, 2001).

2.3.2. Aerosol optical depth variation

The relation of AOD with atmospheric physics and regional air quality is widely discussed, for example, for stating the correlation between cloud condensation nuclei and AOD (Liu & Li, 2014) or the correlations between $PM_{2.5}$ and AOD (Kim, Zhang, Holt, & Liu, 2013). We perform an analysis (with a top-down approach) using AOD data, which could be useful to provide and link information related to the variation of aerosols during the anthropogenic emissions switch-off over five Indian cities. AOD measures aerosol loading, which is an optical property derived from different earth observation satellites (Li et al., 2009). The AOD spatial distribution maps show monthly average aerosol loadings worldwide, whereas the boundary values of optical thickness range from 0 to 1. An optical thickness of 0.1 is characterised by a crystal-clear sky with maximum visibility and an optical thickness of 1 represents very hazy conditions (NASA, 2020a). The analysed AOD datasets in this estimation, which were extracted from the NASA-Earth Observatory Global maps webpage (https://earthobservatory.nasa.gov/global-maps), included both Terra- and Aqua-MODIS (Moderate Resolution Imaging Spectroradiometer) with a resolution of 0.1° × 0.1°. The Terra- and Aqua-MODIS instruments scan the same area of Earth, with three-hours apart (NASA, 2020b). According to the Space Science and Engineering Centre (SSEC, 2020a), the Terra satellite crossing times in India (local time) approximately range from 0900 to 1100 h and from 2100 to 2300 h. For the Aqua satellite, approximate crossing times are from 0100 to 0300 h and from 1200 to 1400 h (SSEC, 2020b). For this study, a comparison analysis was carried out on monthly averaged AOD of both Terra- and Aqua-MODIS datasets during the lockdown period. March 2020 (before-lockdown) and April 2020 (during-lockdown) were selected as the reference periods for the analysis. The comparison analysis was obtained by means of the AOD variation, calculated as follows:

$$AOD_{variation} = [(AOD_i - AOD_{ref}) / AOD_i] \times 100 \quad (2)$$

where AOD_i and AOD_{ref} represent a comparison month (during-lockdown) and the reference month (before-lockdown), respectively.

2.3.3. Health impact assessment and economic valuation

Impacts of reduced $PM_{2.5}$ pollution, such as averted health burden (HB, in terms of premature deaths) related to $PM_{2.5}$ exposure reductions and associated economic outcomes, have attracted worldwide attention, as summarised in Table S6. We have undertaken health impact assessments and economic valuations regarding $PM_{2.5}$ concentration reductions via a two-step approach: firstly, by estimating HB (Eq. 3) and the excess risk (ER) of premature mortality (Eq. 6); and secondly, by determining the value of associated economic cost (million USD per year) for the selected Indian cities during lockdown (25 March to 11 May 2020), as compared to similar periods of 2015–2019.

HB due to short-term exposure to $PM_{2.5}$ (number of premature deaths; Eq. 3) was estimated for the lockdown period (HB_{LP20}; 25 March to 11 May 2020) and for the lockdown equivalent period during 2015–2019 ($HB_{LEP15-19}$). The reduction in health burden (ΔHB), based on averaged daily mean $PM_{2.5}$ concentrations, is calculated as a difference of the former and latter HB estimates (Eq. 4), following the approach applied in previous studies (Sahu & Kota, 2016; Chen et al., 2020; Sharma et al., 2020; Venter et al., 2020). Likewise, the potential health benefits due to changes in daily mean $PM_{2.5}$ concentrations (averaged over the lockdown, 25 March to 11 May 2020, and over the lockdown equivalent period of each previous year from 2015) in each city were estimated using the relative risk (RR) and ER associated with the pollutant loads (Eqs. 5 and 6).

$$HB = BM \times Pop \times AF;\ where\ AF = (RR-1)/RR \tag{3}$$

$$\Delta HB = HB_{LEP15-19} - HB_{LP20} \tag{4}$$

$$RR_{PM2.5} = exp[\beta_{PM2.5} \times (C_{PM2.5} - C_{PM2.5,0})],\ C_{PM2.5} > 0 \tag{5}$$

$$ER = RR-1 \tag{6}$$

where BM (baseline mortality per 100,000 people of all age groups) was obtained from standardised baseline mortality rates (Table S6) published by the Global Burden of Disease study of 2017 (GBD, 2017). Exposed population (Pop) was estimated by applying a 76.8% factor to the city-wise population of each Indian city. This factor was obtained from the Global Burden of Disease study for India (Balakrishnan et al., 2019), whereby the authors estimated this fraction when the total Indian population was assumed to be exposed to National Ambient Air Quality Standards for $PM_{2.5}$. AF (attributable fraction) of a specific RR (Eq. 5; Table S7) is associated with pollutant load. β is the exposure-response coefficient indicating the additional health risk (such as mortality) caused per unit of $PM_{2.5}$, when concentrations exceed a threshold limit. For example, the β value is considered to be 0.038% for $PM_{2.5}$ per μg m^{-3} (Hu, Ying, Wang, & Zhang, 2015; Shen et al., 2020). $C_{PM2.5}$ is the daily mean $PM_{2.5}$ concentration with reference to the threshold concentration ($C_{PM2.5,0}$ of 0 μg m^{-3}), which means that concentrations below or equal to this value are associated with no excess health risk (i.e. RR = 1) (Chen et al., 2020).

In the second step, the economic cost was estimated using the value of statistical life (VSL; USD per person) for India. The VSL is based on an individual's valuation of their willingness to pay to reduce the risk of dying, a standard concept used widely (e.g. Xie, Dai, Dong, Hanaoka, & Masui, 2016, 2019, and Etchie et al., 2017) for cost-benefit analyses to reduce air pollution (OECD, 2014; WHO, 2015). The VSL estimate for India is derived from Ghude et al. (2016) as 1.1 million USD per average human lifespan, which is assumed to be the same for the studied period here. The total reduction in HB (per thousand) per city is multiplied by VSL to monetise averted economic cost in billion USD. The value for VSL used in this study is slightly higher than the conservative estimate (USD 602,000) reported by the Organisation for Economic Co-operation and Development for 2010 (OECD, 2014).

The assumptions used for the above analysis were: (1) a uniform RR value was assumed for the city-wise population and did not derive age group and cause-specific RR values for $PM_{2.5}$; (2) state-wise baseline mortality rates were applied to corresponding cities for estimating city-wise HB obtained from the Global Burden of Disease study (GBD, 2017); (3) data from a certain period (25 March to 11 May) was considered to represent lockdown duration and lockdown equivalent periods from previous years (2015–2019), while such analyses are generally conducted with much more comprehensive datasets with an extensive time domain.

3. Results and discussions

3.1. Overview of $PM_{2.5}$ during the lockdown in Indian cities

Table 2 presents the descriptive statistics of five Indian cities during the lockdown period (25 March to 11 May 2020) with respect to similar periods of the past five years, which also minimises the impacts of meteorological conditions on temporal characteristics of ambient $PM_{2.5}$ concentrations. The lockdown restrictions reduced the hourly average concentration of $PM_{2.5}$ in all five cities. For example, $PM_{2.5}$ concentrations during lockdown were 13 ± 10 μg m^{-3} (Chennai), 40 ± 24 μg m^{-3} (Delhi), 31 ± 11 μg m^{-3} (Hyderabad), 29 ± 17 μg m^{-3} (Kolkata) and 28 ± 11 μg m^{-3} (Mumbai), which were reduced by 32, 52, 26, 24 and 10% when compared with those of the same period in 2019 in each city, respectively. These improvements varied when compared with different years from 2015 to 2019, ranging from –19 to –43% (Chennai), –41 to –53% (Delhi), –26 to –54% (Hyderabad), –24 to –36% (Kolkata), and –10 to –39% (Mumbai). Most cities showed an improvement from one-fifth to halving their concentrations during the lockdown period. Moreover, the maximum concentration peak in each city decreased appreciably (up to a 5-fold decrease) during the lockdown period when compared against previous years (Table 2).

Delhi consistently exhibited the greatest improvements against previous years because Delhi, compared to other Indian cities, has a higher number of ordinarily on-road vehicles (Table S1), use of which was restricted during the lockdown period. Delhi has three coal-fired thermal power plants in and around it that had no restrictions on their operation during the lockdown period, in order to meet the energy demands of the city. On a relative basis, it is expected that the emissions of power plants may have similarly influenced $PM_{2.5}$ concentrations during the lockdown in 2020 and the lockdown-equivalent period in 2019. Source apportionment studies for Delhi suggest that the major sources of $PM_{2.5}$ are secondary aerosols (~21%), soil-dust (~21%), vehicle emissions (~20%), biomass burning (14%), fossil-fuel combustion (~14%), industrial emissions (~6%) and sea-salt (~4%) (Sharma, Mandal, Jain, Sharma, & Saxena, 2016). While the effect of reduction in traffic emissions during the lockdown is evident (Fig. S1), switching off the other sources, such as fine mineral/soil dust linked to road-traffic and construction activities and industrial emissions that are also precursors of secondary aerosol formation, may have contributed to the reduced concentrations observed in Delhi. This means that reductions in $PM_{2.5}$ concentrations during lockdown may also be attributed to reduced levels of co-pollutants such as NO_2 and SO_2 levels (Table 1), which play an important role in the formation of secondary aerosols (Chen et al., 2019). Additionally, the effect of emissions from crop residue burning around Delhi has been often linked with pollution episodes in winter (Hama et al., 2020; Kanawade et al., 2020). Stubble burning of wheat residue also occurs in surrounding states of Delhi during pre-monsoon season, including April and May (Nair et al., 2020), which is also the period of the lockdown considered in this work. However, unlike rice crop residue, which is usually not utilised to feed animals and consequently burnt during winters, the wheat crop residue during pre-monsoon seasons is mostly stocked and utilised to feed domestic animals throughout the year (Kanawade et al., 2020). Moreover, dispersion conditions during April and May are expected to be better than during the winter. While such contributions during the lockdown period in Delhi are expected to be minimal, detailed source apportionment studies coupled with regional-scale dispersion modelling are needed to accurately confirm and quantify the contributions of crop residue burning during these months.

It is interesting to note that despite the lockdown, Mumbai recorded the least reductions. Mumbai is a coastal city, and unlike landlocked cities such as Delhi, may benefit from the flushing of city emissions by sea breezes (Kumar et al., 2015). Recent source apportionment studies suggest that $PM_{2.5}$ concentrations in Mumbai are dominated by anthropogenic sources (Police, Sahu, Tiwari, & Pandit, 2018), including

Table 2
Overview of summary statistics of hourly $PM_{2.5}$ concentration for five cities during lockdown period (25 March to 11 May 2020) for each year. *n* is the number of hourly averaged concentration data points for the above-noted duration after cleaning the data (Section 2.3). We estimated p-value using t-tests based on the hourly $PM_{2.5}$ dataset for each year and they were found to be statistically significant (p-value < 0.0001).

Cities	Year	2020	2019	2018	2017	2016	2015
Chennai	Mean ± SD	13 ± 10	19 ± 13	16 ± 12	23 ± 10	19 ± 11	19 ± 12
	Med (max)	11 (95)	17 (79)	13 (370)	22 (63)	17 (165)	16 (80)
	n	1084	1095	1104	1063	909	923
	ΔC[1] (%)	–	–32	–19	–43	–32	–32
Delhi	Mean ± SD	40 ± 24	84 ± 54	71 ± 43	84 ± 57	85 ± 79	68 ± 45
	Med (max)	34 (195)	71 (519)	63(286)	67 (470)	62 (865)	55 (395)
	n	1152	1150	1145	1068	1150	1144
	ΔC (%)	–	–52	–44	–52	–53	–41
Hyderabad	Mean ± SD	31 ± 11	42 ± 17	54 ± 19	68 ± 26	52 ± 24	53 ± 22
	Med (max)	30 (106)	39 (137)	50 (206)	62 (207)	49 (228)	48 (222)
	n	1142	1142	1066	1017	1123	907
	ΔC (%)	–	–26	–43	–54	–40	–42
Kolkata	Mean ± SD	29 ± 17	38 ± 16	43 ± 16	45 ± 13	42 ± 15	38 ± 19
	Med (max)	25 (107)	36 (115)	40 (138)	44 (172)	39 (102)	34 (129)
	n	1151	1149	1031	1075	1121	1125
	ΔC (%)	–	–24	–33	–36	–31	–24
Mumbai	Mean ± SD	28 ± 11	31 ± 16	44 ± 22	46 ± 25	34 ± 19	44 ± 26
	Med (max)	26 (74)	28 (118)	39 (195)	39 (165)	30 (217)	38 (377)
	n	1044	1141	947	980	977	1092
	ΔC (%)	–	–10	–36	–39	–18	–36

[1] $\Delta C = [(C_{2020} - C_{201x})/C_{201x}] \times 100$ is the percent change of average $PM_{2.5}$ in 2020 against the previous years.

crustal material (~9%), sea-salt spray (~6%), coal/biomass combustion (~26%), fuel/oil combustion (~19%), road traffic (~18%) and metal industry (~11%), with and the remainder unknown. During the lockdown, household coal/biomass burning is expected to increase as people spend more time indoors, while most other sources are expected to remain operational and at relatively normal levels. Road traffic and metal industry emissions are expected to decline but constitute less than one-third of total contributions to $PM_{2.5}$ concentrations in Mumbai, possibly explaining a comparatively low impact of the lockdown on observed concentrations.

Despite the switch-off of the majority of commercial/industrial and vehicular emission sources (e.g. –79% and –80% driving in Delhi and Mumbai, respectively, as per Apple mobility trends), which are considered to be dominant sources of emissions in Indian cities (Chen et al., 2020), up to half of the concentration levels remain. This highlights the significance of additional $PM_{2.5}$ sources, such as biomass burning in residential households, roadside waste or municipal solid waste landfills, thermal power plants, electricity generators and regional transport (Hama et al., 2020; Kumar et al., 2013, 2015), and that holistic source-control measures are needed for improved air quality in post-lockdown environments.

3.1.1. $PM_{2.5}$ frequency analysis

Fig. 2 shows the distribution of $PM_{2.5}$ concentrations in different concentration ranges and the peaks during the lockdown, as compared with earlier years in each city, and was carried out using the GEV model (Eq. 1). Additionally, the frequency histograms of $PM_{2.5}$ concentration during lockdown with the fitted density curve are presented in Fig. S2. The PDF of $PM_{2.5}$ concentrations were consistently lower for all cities during the lockdown period, and their shapes are less skewed to the right when compared with the other periods, indicating the expected $PM_{2.5}$ decline due to lockdown restrictions. The extreme $PM_{2.5}$ concentration in the upper tail of the distribution is lower and converges asymptotically to the Gumbel distribution (light tailed). For instance, the GEV model estimated that 1% quantiles of Delhi's $PM_{2.5}$ concentration in the upper tail were 293 μg m^{-3} in the pre-lockdown periods and 135 μg m^{-3} during lockdown, with a 158 μg m^{-3} difference. It also demonstrates that extreme $PM_{2.5}$ (high concentration) values were less frequent during lockdown in all cities, and particularly in Delhi (Fig. 2b). Fig. 2f shows a comparison of $PM_{2.5}$ PDF among all five Indian cities during lockdown. Delhi experienced the greatest benefit, with a ~53% reduction in $PM_{2.5}$ concentrations and more distributed around the central moment.

In order to understand the behaviour of $PM_{2.5}$, mean variation in the distribution of $PM_{2.5}$ concentrations, and the mean difference in $PM_{2.5}$ concentrations during lockdown, the current lockdown period and relative preceding periods at all cities were compared, as listed in Table 3. Among the cities, Delhi showed the highest percentage reduction in $PM_{2.5}$ concentrations (over 50%) and Mumbai had the lowest at about 12%, with a p-value of < 0.01 (1%), which indicates that the percentage of reductions were statistically significant (Table 3). The mean values of $PM_{2.5}$ concentration estimated by the GEV model varied from 20 to 85 μg m^{-3} in the preceding year and 13–40 μg m^{-3} during lockdown in Chennai and Delhi, respectively. The percentage reduction for the other cities ranged from 24 to 32%, which were slightly smaller than the measured values for Delhi and Mumbai. The most frequent (mode) value varied from 2 μg m^{-3} (Chennai) to 28 μg m^{-3} (Delhi) during the lockdown period. The most frequent $PM_{2.5}$ concentration ranges in each city during the lockdown period were: 2−6 μg m^{-3} in Chennai, 21−28 μg m^{-3} in Delhi, 24−27 μg m^{-3} in Hyderabad, 17−19 μg m^{-3} in Kolkata and 19−22 μg m^{-3} in Mumbai. Overall, the GEV model is in agreement with observed $PM_{2.5}$ and properly reproduced the distribution of $PM_{2.5}$ during the two study periods.

3.1.2. Temporal and diurnal trends

Fig. 3 shows a boxplot for $PM_{2.5}$ during the lockdown period for six years for all cities. To further assess the impact of lockdown on $PM_{2.5}$ trends in five major cities, a smoothed time series of 2020 $PM_{2.5}$ concentrations was compared with that of the previous five years (Fig. S3). $PM_{2.5}$ gradually decreased over the lockdown period in all five cities. These observations were more pronounced when the previous five-year average was compared to the lockdown period of 2020 (Fig. S3). While all cities showed greater improvements towards the end of the lockdown period, landlocked cities (Delhi and Hyderabad) reported less than half the $PM_{2.5}$ levels of those of the previous five-year average. Finally, the trend of $PM_{2.5}$ percentage reduction in 2020 compared to the past five years reported similar variations across cities, with fluctuations in the early lockdown period preceding a comparatively steady percentage reduction in $PM_{2.5}$ concentrations as the lockdown continued (Fig. S4).

The diurnal variation of $PM_{2.5}$ during the lockdown period was plotted against 2019 (Fig. 4) and the previous five years (Figs. S5−8)

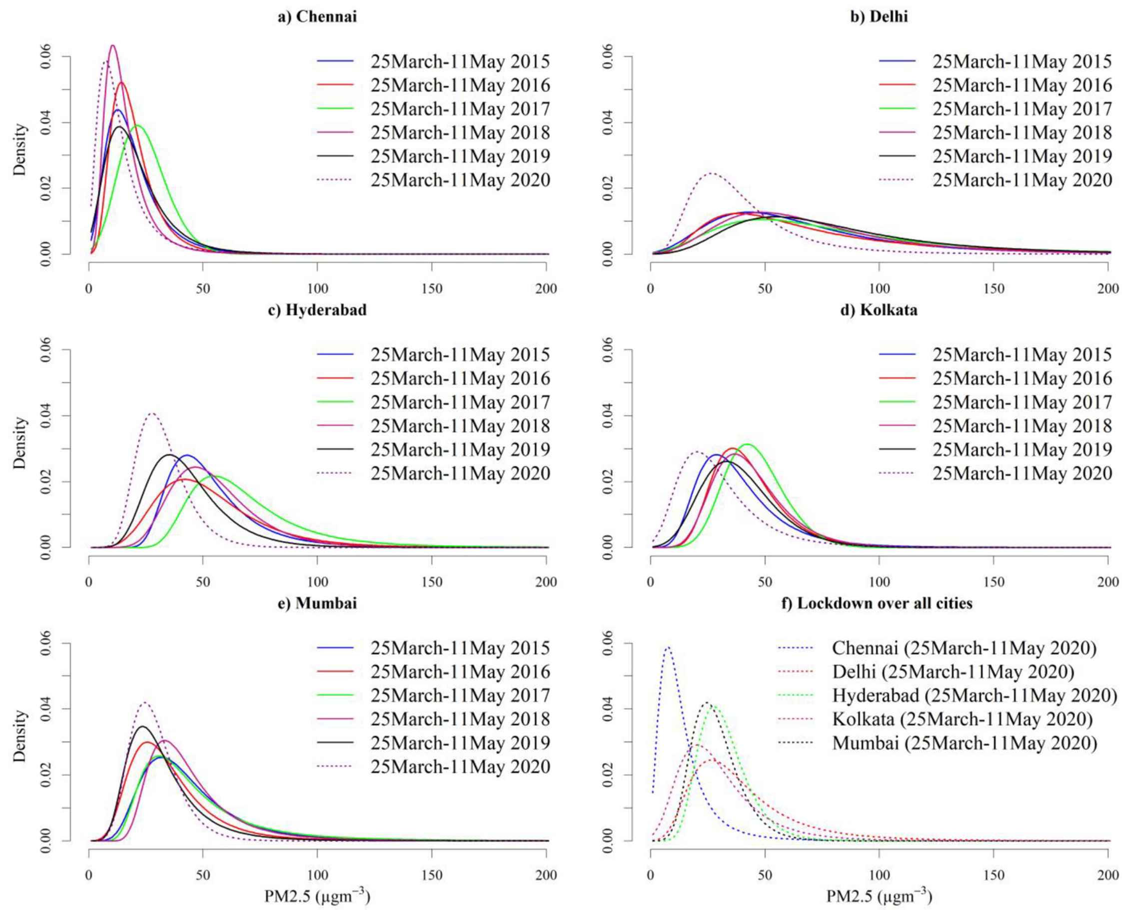

Fig. 2. Density plot of hourly $PM_{2.5}$ concentration before and during lockdown for (a) Chennai, (b) Delhi, (c) Hyderabad (d) Kolkata, (e) Mumbai, and (f) all cities only during the lockdown period.

Table 3
Sample and GEV model estimated means, percentage of mean reduction in $PM_{2.5}$ and p-values before (2019) and during lockdown periods.

City	25 March to 11 May 2019		25 March to 11 May 2020			
	Sample mean (μg m^{-3})	GEV estimated mean (μg m^{-3})	Sample mean (μg m^{-3})	GEV estimated mean (μg m^{-3})	% of mean reduction (2019 – 2020)	p-value
Chennai	20	20	13	13	32	2.2e^{-16}
Delhi	84	85	40	40	53	2.2e^{-16}
Hyderabad	42	42	31	31	26	2.2e^{-16}
Kolkata	38	38	29	29	24	2.2e^{-16}
Mumbai	31	31	28	28	12	1.5e^{-09}

for all cities to show the impact of lockdown on $PM_{2.5}$ levels. Lockdown implementation flattened the diurnal $PM_{2.5}$ concentration trend in all cities (Fig. 4). Most of the $PM_{2.5}$ peaks observed during daytime (0600 – 1800 h) were less prominent in 2020 when compared with previous years in all cities, indicating fewer anthropogenic activities as discussed above. The maximum comparative reduction in $PM_{2.5}$ concentrations during lockdown was noted to occur at around 0900 h, coinciding with morning traffic peak hours.

In order to further understand $PM_{2.5}$ trends during lockdown, average daily $PM_{2.5}$ concentrations were normalised using average daily $PM_{2.5}$ preceding 23 March 2019 (Fig. 4) and the previous years as reference values (Figs. S5 – 8). In all cities except Delhi, $PM_{2.5}$ concentrations gradually reduced during the studied period in all six years when compared to the preceding reference day, and the ratio was further lowered towards the end of study period. In Delhi, however, 2020 $PM_{2.5}$ concentrations were unchanged when compared to preceding reference days (Ratio = 1) while higher $PM_{2.5}$ concentrations were recorded in previous, non-lockdown years.

3.2. Lockdown impact on $PM_{2.5}$ across cities

In order to understand the spatial variation of declines in $PM_{2.5}$ concentrations during lockdowns in cities across the world, a review of recent relevant studies was undertaken (Table S8), visualisation of which is presented in Figs. 5 and 6. The Indian cities studied here showed a significant impact of lockdown on air quality. For example, Delhi saw a reduction of up to 52% in average $PM_{2.5}$ concentration when compared with the same time period of the previous year (Table 2). These reductions were expected due to enforced self-isolation and restricted daily activities, with inevitably reduced emissions from traffic and industrial sources (Section 3.1). Our estimated $PM_{2.5}$ reduction was greater for Delhi (-52%) than the -39% reported by Mahato

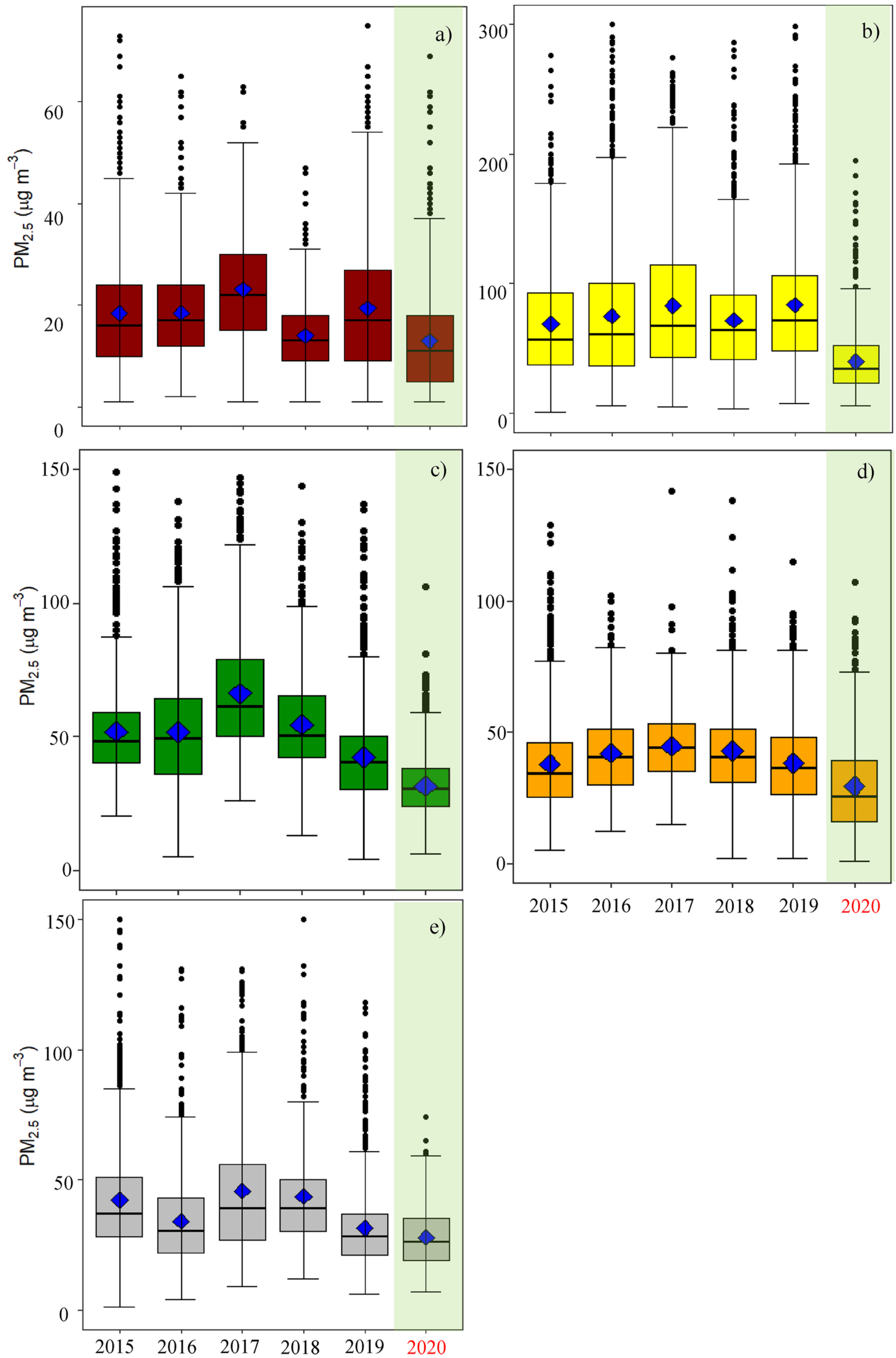

Fig. 3. Variability of $PM_{2.5}$ concentrations (µg m^{-3}) during lockdown period (25 March to 11 May 2020) for (a) Chennai, (b) Delhi, (c) Hyderabad, (d) Kolkata, and (e) Mumbai. The plot represents the mean $PM_{2.5}$ (diamonds), the median (horizontal bars in the centre of boxes), the 25th and 75th percentiles (the bottom and top edge of the boxes), and minimum and maximum concentration (the bottom and the top edge of the whiskers). The plot also shows extreme observations, which are much larger and lie above the rest of the data as black dots).

et al. (2020) and -35% by Chauhan and Singh (2020), and was also slightly higher for Mumbai (-14%) than the -10% reported by Chauhan and Singh (2020). This may be attributed to the greater duration of lockdown considered by our study (Table S8). Indeed, other cities across the world, such as Paris (-53%), Amsterdam (-47%) and London (-45%), have shown similarly marked declines in $PM_{2.5}$ concentrations (Shrestha et al., 2020). Kolkata, Hyderabad and Chennai saw 22, 26 and 28% reductions in $PM_{2.5}$ concentrations, respectively. These results are

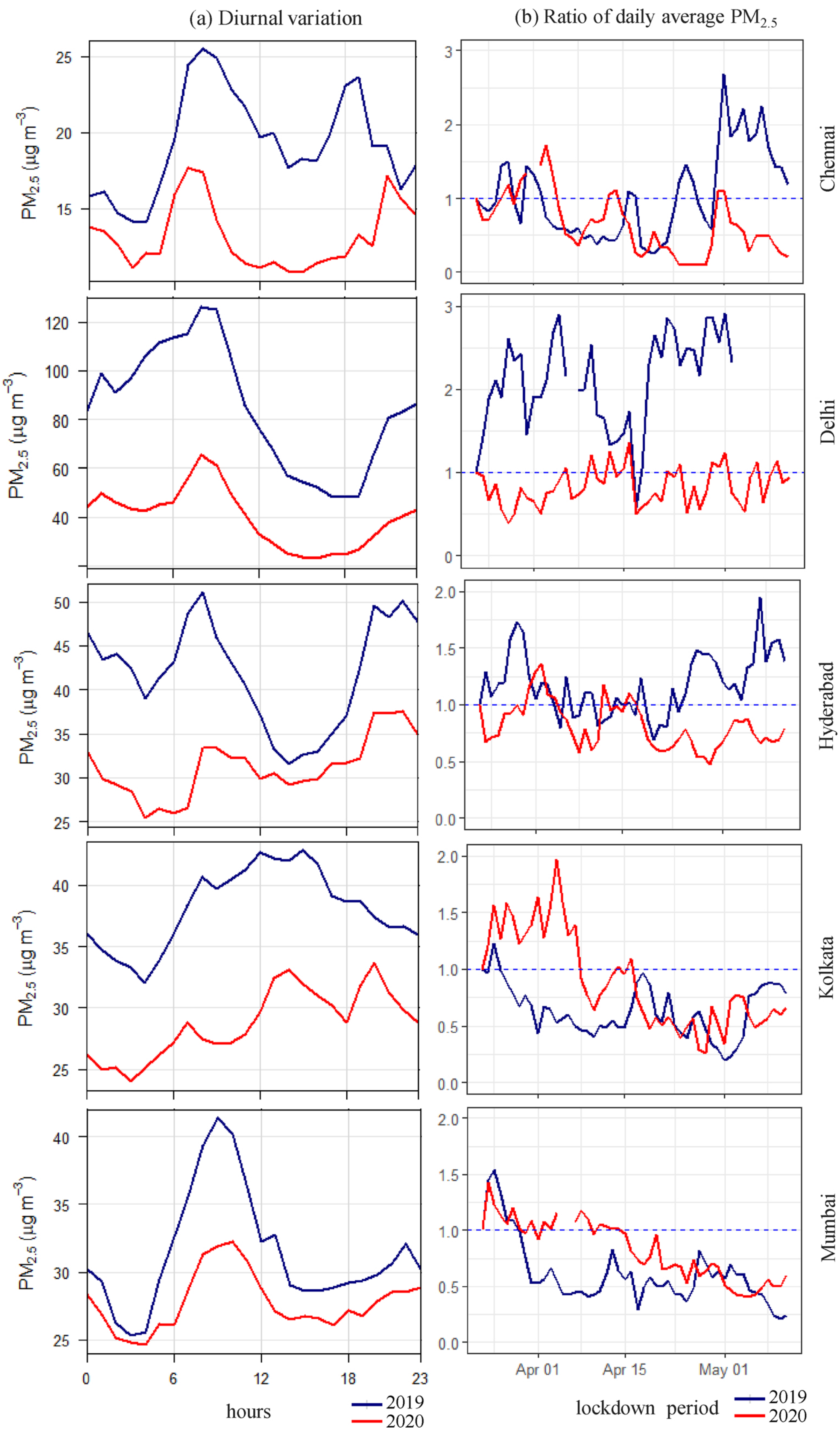

Fig. 4. (a) Diurnal variation of $PM_{2.5}$ during lockdown period in 2019 (blue) and 2020 (red) at five Indian cities; and (b) daily change in relative concentrations of $PM_{2.5}$ during lockdown period in 2019 (blue) and 2020 (red) against the daily average concentration on 25 March of corresponding years. The broken lines show missing datasets.

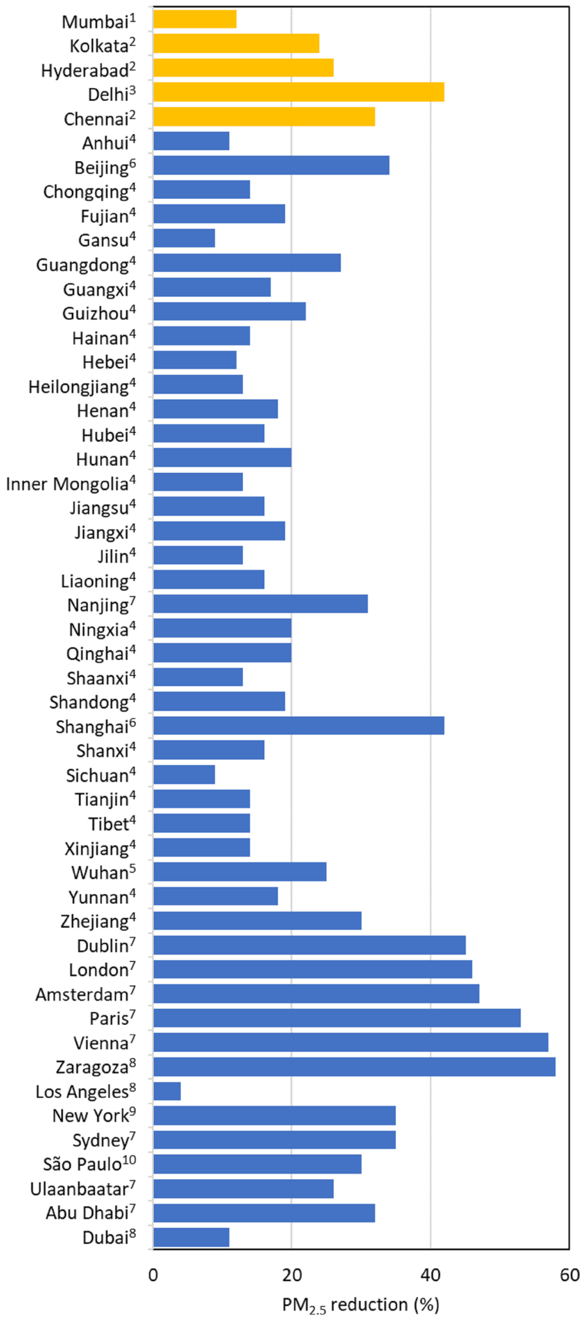

Fig. 5. $PM_{2.5}$ concentration reduction in percentage due to COVID-19 lockdown in various global cities during Feb-May 2020 compared to the same period in previous years (Table S8). The cities considered in this study are shown in orange. Source: [1]Average of this study and Chauhan and Singh (2020); [2]This study; [3]Average of this study, Mahato et al. (2020) and Chauhan and Singh (2020); [4]Huang et al. (2020); [5]Zambrano-Monserrate et al. (2020); [6]Average of Huang et al. (2020) and Chauhan and Singh (2020); [7]Shrestha et al. (2020); [8]Chauhan and Singh (2020); [9]Average of Shrestha et al. (2020) and Chauhan and Singh (2020); [10]Nakada and Urban (2020).

very similar to those for other Asian cities, such as Hunan, Guangdong and Guizhu of China, with $PM_{2.5}$ reductions ranging between 20% and 30% (Table S8). Delhi's nearly 50% reduction in $PM_{2.5}$ is very similar to results from studies into two other Asian megacities: Shanghai and Beijing (Chauhan & Singh, 2020). In general, relatively large reductions were seen for high-population cities because anthropogenic $PM_{2.5}$ emissions are typically higher in these cities during normal working days than in smaller and less urbanised cities or towns (Zhao et al., 2009).

$PM_{2.5}$ concentration reductions due to lockdown have varied in different cities across the world (Fig. 5). Minimal reductions were seen in Rome, where there has been little change in the volume of traffic, a primary source of $PM_{2.5}$ in Rome (Dimitriou & Kassomenos, 2014), and in the city centre of Sao Paulo, where public transportation continued during a partial lockdown (Nakada & Urban, 2020). In China, estimated $PM_{2.5}$ reductions vary from a minimum of 9% in Sichuan to a maximum of 50% in Beijing and Shanghai, due to differences in levels of urbanisation and in the timing of halts in human activities (Huang et al., 2020). Meteorology also plays a significant role in pollution dispersion, and rain or storms during the study period may have enhanced dispersion and deposition (Yang, Yao, Li, & Fan, 2013). For example, in the US, New York experienced a ~35% reduction, compared with only 4% in Los Angeles, due to rainfall over the lockdown period (Chauhan & Singh, 2020). However, the effect of lockdown on air quality is perceptible in most cities of the world. While the intensity of anthropogenic pollutant sources (discussed in Section 3.1), their switch-off period, lockdown strictness and local meteorological conditions were all influencing factors for variation in the impact of lockdowns on $PM_{2.5}$ across cities (Fig. 6), changes in on-road traffic was one clear and major factor. This substantiates our earlier observation (Section 3.1) that decreasing traffic volume showed a proportionally decreasing trend in $PM_{2.5}$ concentrations (Fig. S1), explaining why cities with higher vehicular populations tend to show higher reductions in $PM_{2.5}$ concentrations during lockdown, when transportation activities were restricted.

3.3. Spatial distribution of AOD

We used the AOD index to analyse whether an increase or decrease of aerosol loadings in Indian cities was related to the lockdown. The AOD index at 0.1° pixel of regional scale offers a different perspective regarding the complexity involved in the spatial distribution of aerosol loadings. It also enables visualisation of aerosol hotspots globally, regionally or for a specific city. To do so, we generated 12 AOD maps equally covering the months of March and April of each year from 2015 to 2020 (Figs. S9 – 10). These maps were compared in terms of AOD variation (Section 2.3.2) for all the studied Indian cities.

Fig. 7 shows the spatial distribution of AOD over India and across all five cities before and during lockdown (March and April 2020). It is known that AOD is related to topography (Fig. 1), with maximum values usually found in lowlands (Dong et al., 2013). We observed a similar pattern in the before-lockdown period and during previous years (Fig. 7a–c). However, as expected, an opposite pattern was seen for the during-lockdown period (Fig. 7d), implying a decrease in aerosol loadings in these lowland cities. The spatial distribution of AOD during March 2019, April 2019 and March 2020 is shown in Fig. 7a–c, where values in the 0.4 – 0.8 range can be observed in northern India and 0.6 – 0.8 in northeast India. Conversely, these values were in the 0.2 – 0.4 range during April 2020 (Fig. 7d) in northern India, with a reduction in aerosol loadings mirroring the lockdown period.

The AOD variations demonstrated an increase or a decrease in aerosol loadings in different regions of India. The AOD variation for March 2020 compared to March 2019 (Fig. 8a) shows an increase (20–100%) in aerosol loadings in north India. Conversely, April 2020 (Fig. 8b) saw a decrease in north, east and south India, which could be linked to the lockdown. The AOD variation results are in line with those reported by Sharma et al. (2020), who found the highest air quality index (AQI) reductions in north (44%) and south (33%) India and the lowest in central India (15%), where AOD variation showed high spatial-horizontal variation.

AOD variation in five Indian cities during March and April 2020 was compared against that of previous years (Fig. 9). When compared to data from 2019, a reduction in aerosol loadings in Hyderabad (5%) and

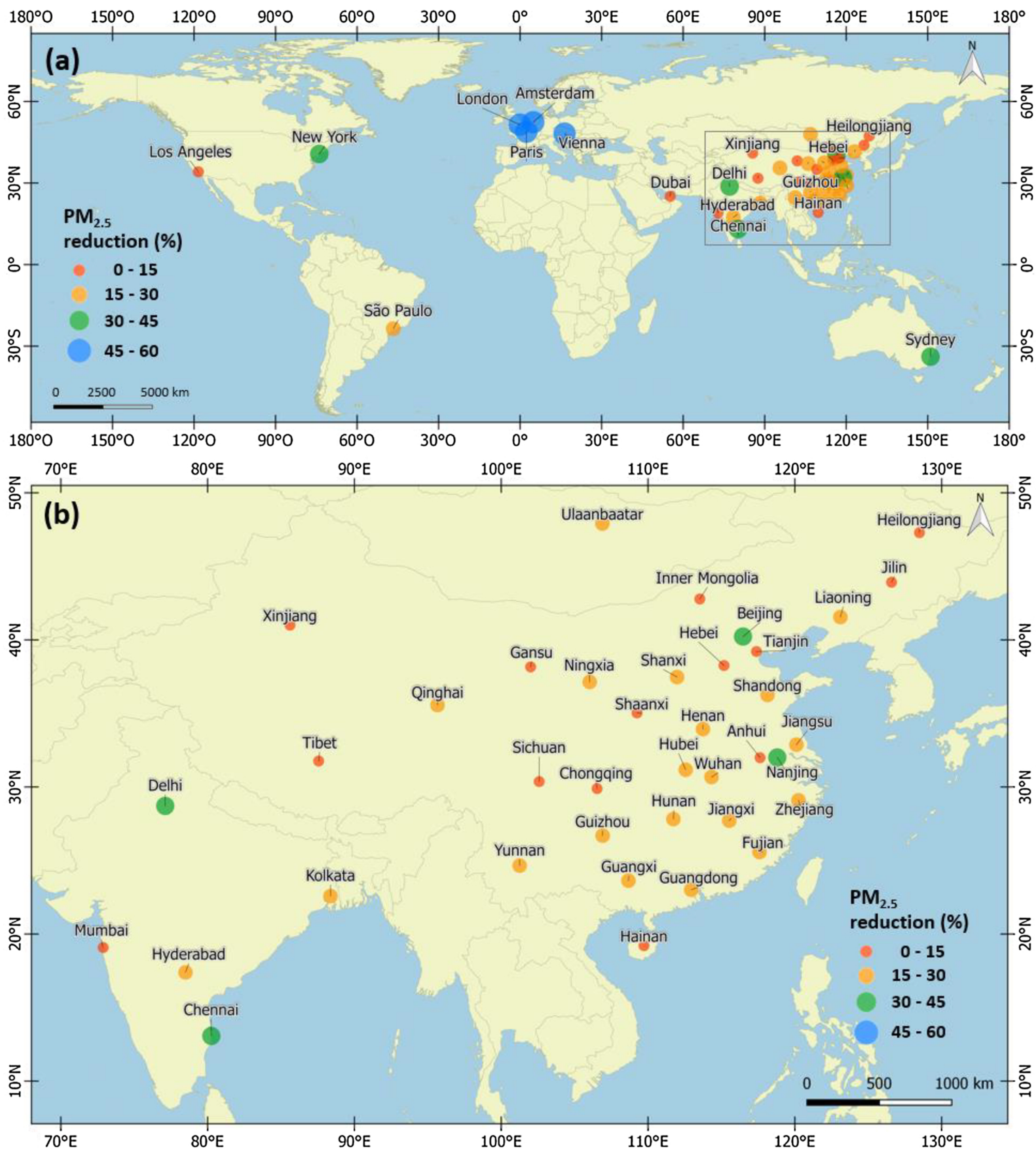

Fig. 6. Decline in $PM_{2.5}$ concentration in percentage due to COVID-19 lockdown in various cities across the world during Feb-May 2020 compared to the non-lockdown period in the past (Table S8). Declines in Mumbai, Delhi, Beijing, Shanghai and New York are from the average of different studies, as noted in Fig. 5 and also detailed in Table S8.

an increase in Mumbai (57%) was observed for the before-lockdown period (March 2020; Fig. 9a). These fluctuations in the form of a city-specific decrease or increase could be related to other regional inputs/outputs, such as commercial/industrial emissions and meteorological conditions. It is worth noting that AOD variation can be large and that differences can be complex at regional scale, and the same applies for aerosol properties (Li et al., 2009). Conversely, during lockdown (April 2020), as presented by Fig. 9b, a reduction in aerosol loadings was observed for Chennai (29–57%), Delhi (11–29%), Kolkata (2–14%) and Mumbai (1–48%). However, Hyderabad showed fluctuations, with an increase of 25% in aerosol loadings in April 2020 compared to 2019, and a decrease of 8% with respect to 2018.

The AOD relationship with topography was not seen to continue during the lockdown period, particularly in north India, showing a different pattern to that of previous years (Fig. S11). Furthermore, four cities (Chennai, Delhi, Kolkata, and Mumbai) showed an AOD decrease in line with the analysis performed in Section 3.2. However, Hyderabad showed an AOD increase, which is not in line with the reduction discussed in Section 3.2. This variation may be partly related to the different resolution of the dataset involved in this work (e.g. monthly AOD data used here and hourly data used in Section 3.2). Due to the 'switch-off' of most commercial/industrial and vehicular emissions, the AOD increase may also be attributable to other sources related to regional conditions. Some regional sources that may have contributed include cloud formation in late-afternoon to evening hours and mineral dust transport (from the Thar Desert) during the pre-monsoon period (March-May) (Kaskaoutis, Badarinath, Kumar Kharol, Rani Sharma, & Kambezidis, 2009). These topographical and geographical characteristics illustrate that not only anthropogenic but also natural emissions are important sources in this region.

3.4. Averted health burden and associated economic cost

We quantified the health and economic impacts of lockdown-

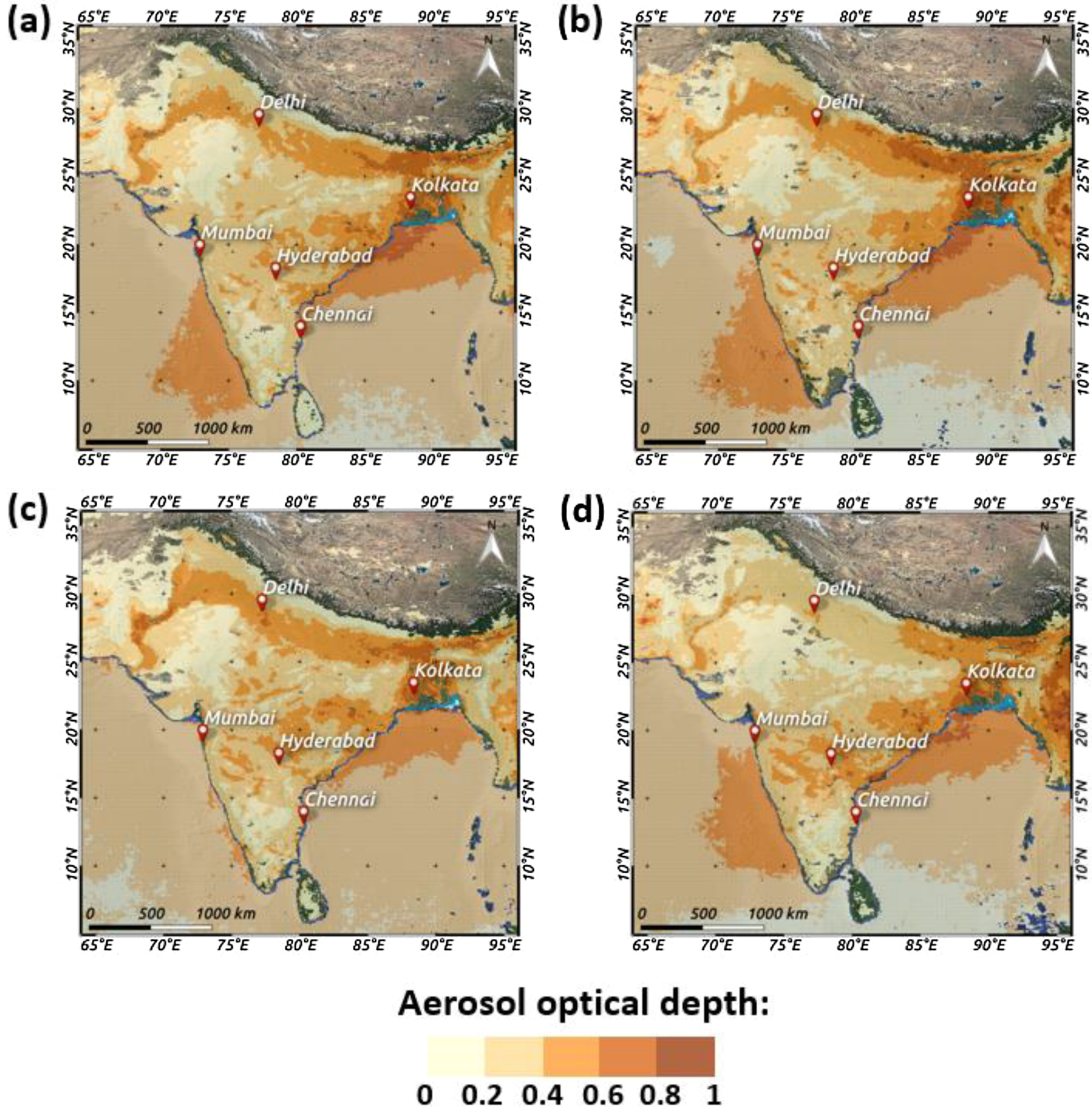

Fig. 7. Spatial distribution of AOD over India: (a) March-2019, (b) March-2020, (c) April-2019, (d) April-2020.

induced reductions in $PM_{2.5}$ concentrations across selected Indian cities (Fig. 10 and Table S9). The health impacts are presented in terms of ER and averted HB (i.e. reduced number of premature deaths) associated with daily mean $PM_{2.5}$ exposure during periods with lockdown (HB_{LP20}) and without lockdown ($HB_{LEP15-19}$). The mean daily ER reduced by 36.4% over all five cities, with 30, 50, 42, 30 and 30% reductions in Chennai, Delhi, Hyderabad, Mumbai and Kolkata when compared with the previous five years, respectively (Table S9). The reduction in ER during lockdown was greatest for Delhi (20% greater than Chennai, Mumbai and Kolkata, and 8% greater than Hyderabad) when compared with similar periods of previous years. The mean ER averaged across the five Indian cities (36%) was lower than the 52% value reported by Sharma et al. (2020), who estimated PM-related risk reduction between 16 March and 14 April 2020 by comparing against the same duration in 2017 − 19 in 22 cities of different regions of India. The reduction in HB during lockdown, as compared against lockdown equivalent periods of the previous five years, was greatest for Delhi (49%) and exceeded Chennai, Hyderabad, Mumbai and Kolkata by 19, 8, 19 and 20%, respectively. Combined estimates for all cities indicates that a total of 630 premature deaths have been avoided across five cities during the lockdown period. These estimates of avoided premature deaths due to $PM_{2.5}$ are within the 12% range of the averaged estimate of 5300 (1000–11700) for India during the first two weeks of lockdown (February/March 2020) as compared to similar periods of 2017 − 2019, conducted by Venter et al. (2020). However, these differences may be linked to variations in the considered time domain and number of cities.

The averted HB, using the principle of VSL (Section 2.3.3), is monetised at 0.69 billion USD (Table S9). In other words, during the 2020 lockdown period, India benefited by as much as 0.69 billion USD, which is 14% of India's total allocated healthcare spending for the fiscal year 2020–2021 (i.e. 5.09 billion USD). This is also roughly 11% higher than India's planned outlay (USD 622.78 million) towards the environment and climate change as per the Indian Union Budget for the financial year 2020 − 21 (IBEF, 2020). Additionally, a linear correlation (R^2 = 0.84) between changes in prevented premature deaths and averted economic cost was observed among all cities, which may support the economic value of lockdown restrictions. However, this analysis does not infer or endorse lockdown as a strategy to promote sustainable development but merely highlights the potential health and associated economic co-benefits of reduced business activities and human mobility. The analysis does not account for COVID-19 lockdown impacts on other macroeconomic indicators, such as gross domestic

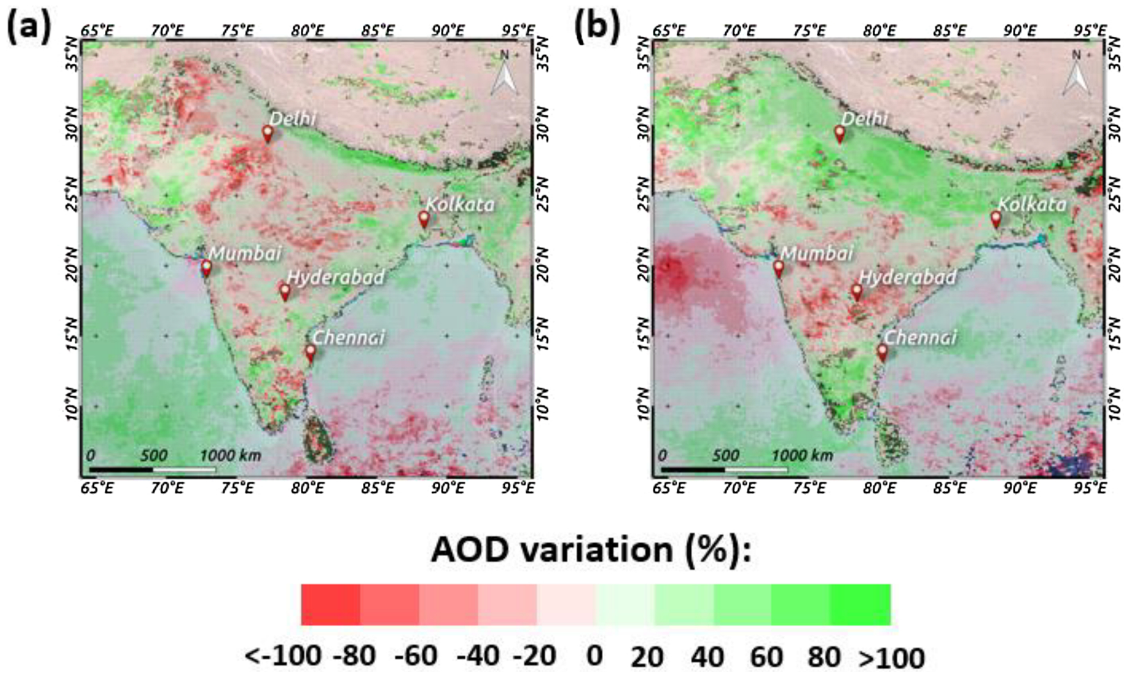

Fig. 8. AOD variation over India for: (a) March 2020 compared to March 2019; (b) April 2020 compared to April 2019. Decrease and increase in aerosol loadings are shown as green- and red-shaded regions, respectively.

product, inflation or employment, which might have much more serious and wider implications for the Indian economy (Barua, 2020). In particular, restrictive measures during lockdown have disproportionately affected the livelihood and socio-economic activities of poorer communities (Buheji et al., 2020). Nevertheless, such analyses may contribute towards an understanding of the annual health and economic impacts of lockdown, to support a holistic assessment of impacts and inform relevant policy measures.

4. Conclusions

We studied the impact of the 'anthropogenic emissions switch-off' during COVID-19 lockdown on ambient $PM_{2.5}$ in five Indian cities, by comparing 2020 data with that of preceding years and contextualising our results with those from other cities. We also analysed the PDF of $PM_{2.5}$, the spatial distribution of AOD using satellite imagery, and health and economic valuations of the impact of decreased $PM_{2.5}$ concentrations. Conclusions include:

- The analysis of relative reductions in $PM_{2.5}$ due to lockdown restrictions showed the highest (52%) and lowest (10%) reductions for Delhi and Mumbai, respectively, as compared against the same period in 2019. Chennai (32%), Hyderabad (26%), and Kolkata (24%) also showed promising reductions over similar periods. Although the correlation between $PM_{2.5}$ concentrations and the decrease in vehicular traffic across these cities was found to be linear ($R^2 = 0.69$), the potential contribution of commercial/industrial sectors and other $PM_{2.5}$ sources (biomass burning in residential households, thermal power plants, electricity generators, and secondary particle formation) are also considered to be impactful.
- During the lockdown period, extreme $PM_{2.5}$ concentrations were less frequent in all five cities. Delhi benefited the most, with a greater than 50% reduction in concentrations, as also estimated by the GEV model. The GEV model also performed well in capturing the distribution and reproducing the mean percentage reduction in $PM_{2.5}$ for the two study periods. Statistically significant p-values (< 0.01) were observed when comparing $PM_{2.5}$ reductions between the current lockdown period and relative preceding periods in all cities, with Delhi showing the highest concentration reductions (over 50%) and Mumbai the lowest (12%). Therefore, the lockdown period affected $PM_{2.5}$ associated risks by reduction of their onset probability, in particular during peak (day) time.
- During the lockdown period, all five cities displayed a gradual decrease in $PM_{2.5}$ concentrations, resulting in greater improvements towards the end of study duration. Analysis of diurnal variation of $PM_{2.5}$ in these cities revealed that the implementation of lockdown helped to suppress $PM_{2.5}$ peaks during the daytime, and especially in the morning, when compared to previous years. Diurnal $PM_{2.5}$ variation showed generally lower concentrations during the lockdown period in 2020 when compared with the same period of previous years.
- Indian cities showed up to 50% reductions (Delhi) in $PM_{2.5}$ concentrations, compared with up to 60% in Europe (Vienna and Zaragoza), and other global cities ranged from 4% in Los Angeles to 42% in Shanghai. The lockdown-induced $PM_{2.5}$ reduction in India was distinct and depended on various factors. Large and densely populated cities with high traffic volumes seemed to correlate with high $PM_{2.5}$ reductions. Other influencing factors included the intensity of other anthropogenic pollutant sources (e.g. indoor), lockdown strictness and duration, and meteorological fluctuations.
- The spatial distribution of AOD during lockdown (April 2020) demonstrated that aerosol loadings decreased in Chennai (29%), Delhi (11%), Kolkata (4%), and Mumbai (1%), with respect to April 2019. AOD variation analysis showed a remarkable reduction in north, east, and south India, with mitigation related to the switch-off of most commercial/industrial and vehicular emissions. Conversely, central India showed an increase in aerosol loadings and high horizontal spatial variation of AOD, which may be linked to different sources (e.g. sea aerosol) or the presence of clouds in the area, potentially leading to an overestimation of AOD.
- An appreciable reduction in daily mean $PM_{2.5}$ concentrations due to lockdown led to a decrease in both ER (30–50%) and EV (29–49%) values, which avoided 630 premature deaths across five Indian cities, valued at 0.69 billion USD. While the reduced levels of air pollution during lockdowns indicate clear health and associated

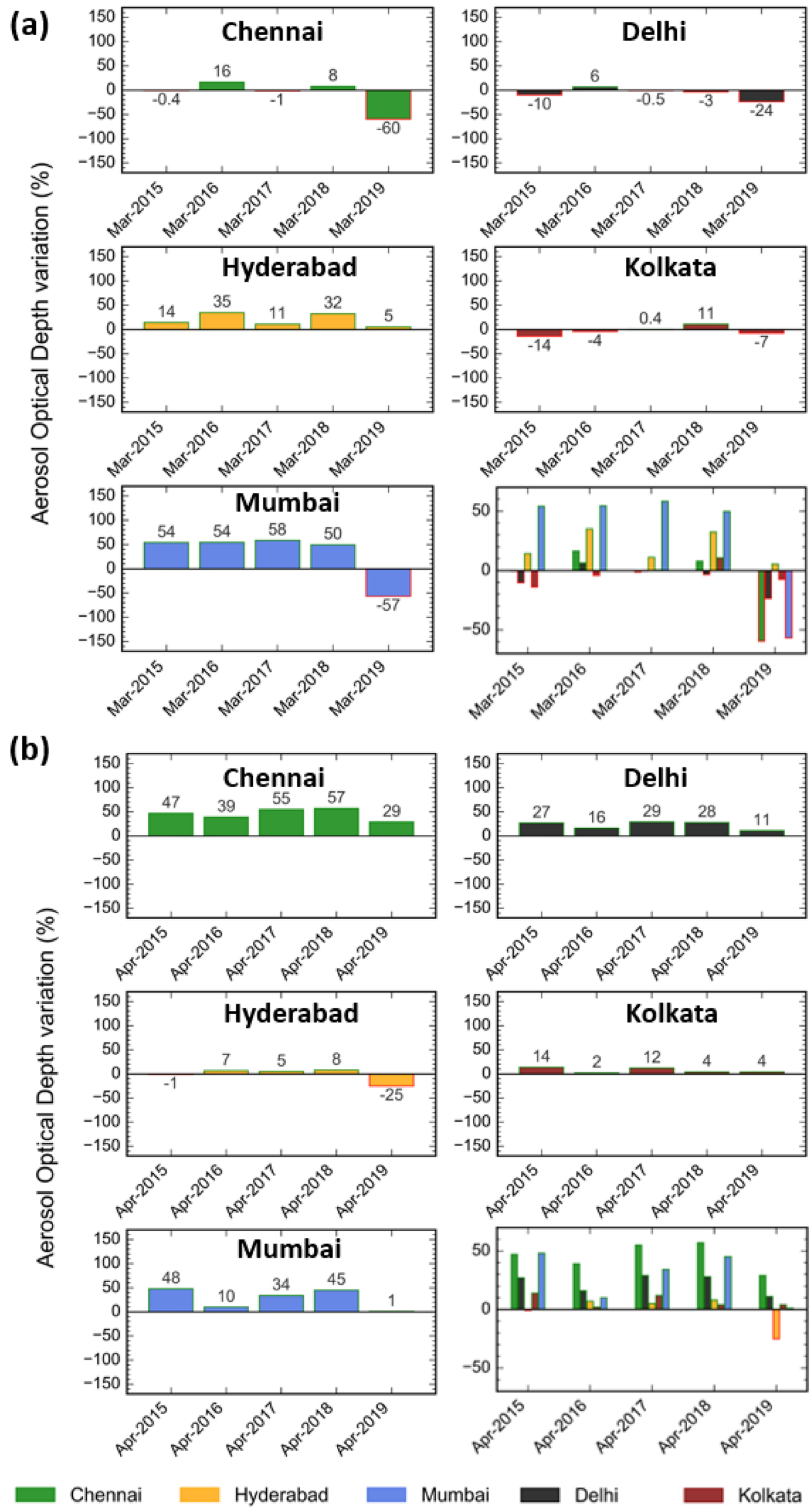

Fig. 9. AOD variation using (a) March 2020 and (b) April 2020 as a reference comparison period, respectively.

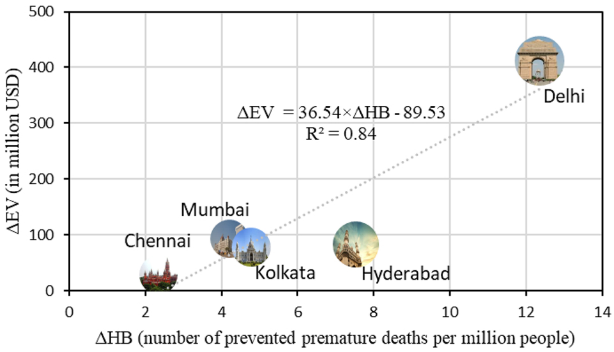

Fig. 10. Distribution of ΔHB versus ΔEV of $PM_{2.5}$ during the lockdown period compared with the previous five years (2015-19) in five Indian cities. Size of circles represents ΔER (%).

economic co-benefits, and that cities should plan more rigorous strategies to control air pollution, we do not infer or endorse such benefits at the cost of such pandemics, which have brought devastating impacts on communities, businesses, economies, human mobility and so on.

We demonstrated a reduction in $PM_{2.5}$ during the COVID-19 lockdown period in Indian cities, similar to reductions seen in cities elsewhere. A multi-pollutant assessment, considering primary and secondary pollutants over a majority of the lockdown period, is recommended for future work to obtain a holistic picture of the impact of lockdown period on air pollutants. Generally, cities with larger traffic volumes showed higher reductions in $PM_{2.5}$ during the lockdown. Our study also highlighted that other emissions sources contributed to a permeation in albeit subnormal $PM_{2.5}$ concentrations during the lockdown period. Source apportionment studies, disentangling the contributions of underpinning operational emission sources, are therefore desirable in order to understand their relative impacts during the 'anthropogenic emissions switch-off' of COVID-19 lockdown.

CRediT authorship contribution statement

Prashant Kumar: Conceptualization, Funding acquisition, Writing - original draft, Resources, Supervision, Project administration, Methodology, Writing - review & editing. **Sarkawt Hama:** Data curation, Methodology, Writing - original draft, Investigation, Validation, Writing - review & editing. **Hamid Omidvarborna:** Writing - original draft, Writing - review & editing. **Ashish Sharma:** Formal analysis, Writing - review & editing. **Jeetendra Sahani:** Formal analysis, Writing - review & editing. **K.V. Abhijith:** Formal analysis, Writing - review & editing. **Sisay E. Debele:** Formal analysis, Writing - review & editing. **Juan C. Zavala-Reyes:** Formal analysis, Writing - review & editing. **Yendle Barwise:** Writing - review & editing. **Arvind Tiwari:** Formal analysis, Data curation, Writing - review & editing.

Declaration of Competing Interest

The authors declare no conflict of interest.

Acknowledgements

The authors acknowledge the support by the NERC funded project, ASAP-Delhi (An Integrated Study of Air Pollutant Sources in the Delhi National Capital Region; Grant No. NE/P016510/1) as a part of the UK-India NERC-MOES Programme on Atmospheric Pollution and Human Health in an Indian Megacity (Delhi); the EPSRC funded project, INHALE (Health assessment across biological length scales for personal pollution exposure and its mitigation; Grant No. EP/T003189/1); and Clean Air Engineering for Cities (CArE-Cities), which is funded by the University of Surrey's Research England funding under the Global Challenge Research Fund (GCRF) programme. The authors thank Komal Shukla for her help with the relevant dataset and inputs to the methodology section.

Appendix A. Supplementary data

Supplementary material related to this article can be found, in the online version, at doi:https://doi.org/10.1016/j.scs.2020.102382.

References

Ahmadi, M., Sharifi, A., Dorosti, S., Ghoushchi, S. J., & Ghanbari, N. (2020). Investigation of effective climatology parameters on COVID-19 outbreak in Iran. *The Science of the Total Environment, 729*, Article 138705.

Balakrishnan, K., Dey, S., Gupta, T., Dhaliwal, R. S., Brauer, M., Cohen, A. J., et al. (2019). The impact of air pollution on deaths, disease burden, and life expectancy across the states of India: the Global Burden of Disease Study 2017. *The Lancet Planetary Health, 3*, 26–39.

Bao, R., & Zhang, A. (2020). Does lockdown reduce air pollution? Evidence from 44 cities in northern China. *The Science of the Total Environment, 731*, Article 139052.

Barua, S. (2020). Understanding coronanomics: The economic implications of the coronavirus (COVID-19) pandemic. *SSRN Electronic Journal.* https://doi.org/10.2139/ssrn.3566477.

Bashir, M. F., Bilal, B. M., & Komal, B. (2020). Correlation between environmental pollution indicators and COVID-19 pandemic: A brief study in Californian context. *Environmental Research, 187*, Article 109652.

Bashir, M. F., Ma, B., Komal, B., Bashir, M. A., Tan, D., & Bashir, M. (2020). Correlation between climate indicators and COVID-19 pandemic in New York, USA. *The Science of the Total Environment, 728*, Article 138835.

Berman, J. D., & Ebisu, K. (2020). Changes in US air pollution during the COVID-19 pandemic. *The Science of the Total Environment, 739*, Article 139864.

Brittain, O. S., Wood, H., & Kumar, P. (2020). Prioritising indoor air quality in building design can mitigate future airborne viral outbreaks. *Cities & Health.* https://doi.org/10.1080/23748834.2020.1786652 In Press.

Buheji, M., da Costa Cunha, K., Beka, G., Mavrić, B., de Souza, Y. L. D. C., da Costa Silva, S. S., et al. (2020). The Extent of COVID-19 Pandemic Socio-Economic Impact on Global Poverty. A Global Integrative Multidisciplinary Review. *American Journal of Economics, 10*, 213–224.

Carslaw, D. C. (2015). *The openair manual–open-source tools for analysing air pollution data. Manual for version, 1(4). Manual for version 1.1-4.* King's College London.

Carslaw, D. C., & Ropkins, K. (2012). Openair — An R package for air quality data analysis. *Environmental Modelling & Software, 27-28*, 52–61.

Chauhan, A., & Singh, R. P. (2020). Decline in $PM_{2.5}$ concentrations over major cities around the world associated with COVID-19. *Environmental Research, 187*, Article 109634.

Chen, Y., Wild, O., Ryan, E., Sahu, S. K., Lowe, D., Archer-Nicholls, S., et al. (2019). Mitigation of $PM_{2.5}$ and ozone pollution in Delhi: a sensitivity study during the pre-monsoon period. *Atmospheric Chemistry and Physics, 20*, 499–514.

Chen, Y., Wild, O., Conibear, L., Ran, L., He, J., Wang, L., et al. (2020). Local characteristics of and exposure to fine particulate matter ($PM_{2.5}$) in four indian megacities. *Atmospheric Environment X, 5*, Article 100052.

Coccia, M. (2020). Factors determining the diffusion of COVID-19 and suggested strategy to prevent future accelerated viral infectivity similar to COVID. *The Science of the Total Environment, 729*, Article 138474.

Coles, S. (2001). *An introduction to statistical modeling of extreme values.* London: Springer ISBN: 1852334592, 2001.

Collivignarelli, M. C., Abbà, A., Bertanza, G., Pedrazzani, R., Ricciardi, P., & Miino, M. C. (2020). Lockdown for COVID-2019 in Milan: What are the effects on air quality? *The Science of the Total Environment, 732*, Article 139280.

COVID-19.in (2020). *Government of India.* (accessed 8 May 2020) https://www.mygov.in/covid-19/?cbps=1.

Dantas, G., Siciliano, B., França, B. B., da Silva, C. M., & Arbilla, G. (2020). The impact of COVID-19 partial lockdown on the air quality of the city of Rio de Janeiro, Brazil. *The Science of the Total Environment, 729*, Article 139085.

de Jesus, A. L., Thompson, H., Knibbs, L. D., Kowalski, M., Cyrys, J., Niemi, J. V., et al. (2020). Long-term trends in $PM_{2.5}$ mass and particle number concentrations in urban air: The impacts of mitigation measures and extreme events due to changing climates. *Environmental Pollution, 263*, Article 114500.

Dhammapala, R. (2019). Analysis of fine particle pollution data measured at 29 US diplomatic posts worldwide. *Atmospheric Environment, 213*, 367–376.

Dimitriou, K., & Kassomenos, P. (2014). Indicators reflecting local and transboundary sources of $PM_{2.5}$ and PM_{COARSE} in Rome - Impacts in air quality. *Atmospheric Environment, 96*, 154–162.

Dutheil, F., Baker, J. S., & Navel, V. (2020). COVID-19 as a factor influencing air pollution? *Environment and Pollution, 263*, Article 114466.

EPA (2009). *Standard operating procedure for the continuous measurement of particulate matter.* US Environmental Protection Agency. (accessed 17 June 2020) https://www3.epa.gov/ttn/amtic/files/ambient/pm25/sop_project/905505_TEOM_SOP_Draft_Final_Sept09.pdf.

EPA (2015). *US Environmental Protection Agency. List of designated reference and equivalent* *methods.* (accessed 10 May 2020) https://www3.epa.gov/ttnamti1/files/ambient/criteria/AMTIC%20List%20Dec%202016-2.pdf.

Etchie, T. O., Sivanesan, S., Adewuyi, G. O., Krishnamurthi, K., Rao, P. S., Etchie, A. T., et al. (2017). The health burden and economic costs averted by ambient $PM_{2.5}$ pollution reductions in Nagpur, India. *Environment International, 102*, 145–156.

Faridi, S., Niazi, S., Sadeghi, K., Naddafi, K., Yavarian, J., Shamsipour, M., et al. (2020). A field indoor air measurement of SARS-CoV-2 in the patient rooms of the largest hospital in Iran. *The Science of the Total Environment, 725*, Article 138401.

GBD (2017). *Global burden of disease study 2017 (GBD 2017) data resources: GHDx.* (accessed 15 May 2020) http://ghdx.healthdata.org/gbd-2017.

Ghude, S. D., Chate, D. M., Jena, C., Beig, G., Kumar, R., Barth, M. C., et al. (2016). Premature mortality in India due to $PM_{2.5}$ and ozone exposure. *Geophysical Research Letters, 43*, 4650–4658.

Guo, H., Kota, S. H., Sahu, S. K., Hu, J., Ying, Q., Gao, A., et al. (2017). Source apportionment of $PM_{2.5}$ in North India using source-oriented air quality models. *Environmental Pollution, 231*, 426–436.

Guo, H., Kota, S. H., Sahu, S. K., & Zhang, H. (2019). Contributions of local and regional sources to $PM_{2.5}$ and its health effects in north India. *Atmospheric Environment, 214*, Article 116867.

Hama, S. M., Kumar, P., Harrison, R. M., Bloss, W. J., Khare, M., Mishra, S., et al. (2020). Four-year assessment of ambient particulate matter and trace gases in the Delhi-NCR region of India. *Sustainable Cities and Society, 54*, Article 102003.

Heal, M. R., Kumar, P., & Harrison, R. M. (2012). Particles, air quality, policy and health. *Chemical Society Reviews, 41*, 6606–6630.

Hu, J., Ying, Q., Wang, Y., & Zhang, H. (2015). Characterizing multi-pollutant air pollution in China: Comparison of three air quality indices. *Environment International, 84*, 17–25.

Huang, X., Ding, A., Gao, J., Zheng, B., Zhou, D., Qi, X., et al. (2020). Enhanced secondary pollution offset reduction of primary emissions during COVID-19 lockdown in China. *EarthArXiv*. https://doi.org/10.31223/osf.io/hvuzy.

Hyndman, R., Athanasopoulos, G., Bergmeir, C., Caceres, G., Chhay, L., & O'Hara-Wild, M. (2019). *Forecasting functions for time series and linear models.* 2019. https://cran.r-project.org/web/packages/forecast/forecast.pdf (accessed 17 June 2020).

IBEF (2020). *Healthcare industry in India, indian healthcare sector, services, india brand equity foundation.* (accessed 17 May 2020) https://www.ibef.org/industry/healthcare-india.aspx.

ICMR-PHFI-IHME (2017). *India: Health of the nation's states-the india state-level disease burden initiative*New Delhi: Indian Council of Medical Research, Public Health Foundation of India, Institute for Health Metrics and Evaluation (2017), https://www.healthdata.org/sites/default/files/files/policy_report/2017/India_Health_of_the_Nation%27s_States_Report_2017.pdf (accessed 16 May 2020).

Isaifan, R. J. (2020). The dramatic impact of Coronavirus outbreak on air quality: Has it saved as much as it has killed so far? *Global Journal of Environmental Science and Management, 6*, 275–288.

Jain, S., & Sharma, T. (2020). Social and travel lockdown impact considering coronavirus disease (COVID-19) on air quality in megacities of India: present benefits, future challenges and way forward. *Aerosol and Air Quality Research, 20*, 1222–1236.

Junger, W. L., & De Leon, A. P. (2015). Imputation of missing data in time series for air pollutants. *Atmospheric Environment, 102*, 96–104.

Junninen, H., Niska, H., Tuppurainen, K., Ruuskanen, J., & Kolehmainen, M. (2004). Methods for imputation of missing values in air quality data sets. *Atmospheric Environment, 38*, 2895–2907.

Kanawade, V. P., Srivastava, A. K., Ram, K., Asmi, E., Vakkari, V., Soni, V. K., et al. (2020). What caused severe air pollution episode of November 2016 in New Delhi? *Atmospheric Environment, 222*, Article 117125.

Kanniah, K. D., Zaman, N. A. F. K., Kaskaoutis, D. G., & Latif, M. T. (2020). COVID-19's impact on the atmospheric environment in the Southeast Asia region. *The Science of the Total Environment, 736*, Article 139658.

Kaskaoutis, D. G., Badarinath, K. V. S., Kumar Kharol, S., Rani Sharma, A., & Kambezidis, H. D. (2009). Variations in the aerosol optical properties and types over the tropical urban site of Hyderabad, India. *Journal of Geophysical Research Atmospheres, 114*, 22204.

Kerimray, A., Baimatova, N., Ibragimova, O. P., Bukenov, B., Kenessov, B., Plotitsyn, P., et al. (2020). Assessing air quality changes in large cities during COVID-19 lockdowns: The impacts of traffic-free urban conditions in Almaty, Kazakhstan. *The Science of the Total Environment, 730*, Article 139179.

Kim, M., Zhang, X., Holt, J. B., & Liu, Y. (2013). Spatio-temporal variations in the associations between hourly $PM_{2.5}$ and aerosol optical depth (AOD) from MODIS sensors on Terra and Aqua. *Health, 5*, 8–13.

Kotnala, G., Mandal, T. K., Sharma, S. K., & Kotnala, R. K. (2020). Emergence of blue sky over Delhi due to Coronavirus disease (COVID-19) lockdown implications. *Aerosol Science and Engineering,* 1–11. https://doi.org/10.1007/s41810-020-00062-6.

Kumar, P., & Morawska, L. (2019). Could fighting airborne transmission be the next line of defence against COVID-19 spread? *City and Environment Interactions*. https://doi.org/10.1016/j.cacint.2020.100033 In Press.

Kumar, P., Jain, S., Gurjar, B. R., Sharma, P., Khare, M., Morawska, L., et al. (2013). New directions: Can a "Blue Sky" return to Indian megacities? *Atmospheric Environment, 71*, 198–201.

Kumar, P., Khare, M., Harrison, R. M., Bloss, W. J., Lewis, A., Coe, H., et al. (2015). New directions: Air pollution challenges for developing megacities like Delhi. *Atmospheric Environment, 122*, 657–661.

Kumar, P., Gulia, S., Harrison, R. M., & Khare, M. (2017). The influence of odd–even car trial on fine and coarse particles in Delhi. *Environmental Pollution, 225*, 20–30.

Lal, P., Kumar, A., Kumar, S., Kumari, S., Saikia, P., Dayanandan, A., et al. (2020). The dark cloud with a silver lining: Assessing the impact of the SARS COVID-19 pandemic on the global environment. *The Science of the Total Environment, 732*, Article 139297.

Li, Z., Zhao, X., Kahn, R., Mishchenko, M., Remer, L., Lee, K. H., et al. (2009). Uncertainties in satellite remote sensing of aerosols and impact on monitoring its long-term trend: A review and perspective. *Annals of Geophysics, 27*, 2755–2770.

Li, L., Li, Q., Huang, L., Wang, Q., Zhu, A., Xu, J., et al. (2020). Air quality changes during the COVID-19 lockdown over the Yangtze River Delta region: An insight into the impact of human activity pattern changes on air pollution variation. *The Science of the Total Environment, 732*, Article 139282.

Li, Y., Qian, H., Hang, J., Chen, X., Hong, L., Liang, P., et al. (2020). Evidence for probable aerosol transmission of SARS-CoV-2 in a poorly ventilated restaurant. *medRxiv* 2020.2004.2016.20067728.

Liu, J., & Li, Z. (2014). Estimation of cloud condensation nuclei concentration from aerosol optical quantities: Influential factors and uncertainties. *Atmospheric Chemistry and Physics, 14*, 471–483.

Liu, Y., Ning, Z., Chen, Y., Guo, M., Liu, Y., Gali, N. K., et al. (2020). Aerodynamic analysis of SARS-CoV-2 in two Wuhan hospitals. *Nature,* 1–6.

Mahato, S., Pal, S., & Ghosh, K. G. (2020). Effect of lockdown amid COVID-19 pandemic on air quality of the megacity Delhi, India. *The Science of the Total Environment, 730*, Article 139086.

Mandal, I., & Pal, S. (2020). COVID-19 pandemic persuaded lockdown effects on environment over stone quarrying and crushing areas. *The Science of the Total Environment, 732*, Article 139281.

Martini, F. M. S., Hasenkopf, C. A., & Roberts, D. C. (2015). Statistical analysis of $PM_{2.5}$ observations from diplomatic facilities in China. *Atmospheric Environment, 110*, 174–185.

Martins, L. D., Wikuats, C. F. H., Capucim, M. N., de Almeida, D. S., da Costa, S. C., Albuquerque, T., et al. (2017). Extreme value analysis of air pollution data and their comparison between two large urban regions of South America. *Weather and Climate Extremes, 18*, 44–54.

Mitra, A., Chaudhuri, T. R., Mitra, A., Pramanick, P., Zaman, S., Mitra, A., et al. (2020). Impact of COVID-19 related shutdown on atmospheric carbon dioxide level in the city of Kolkata. *Science Education, 6*, 84–92.

Morawska, L., & Cao, J. (2020). Airborne transmission of SARS-CoV-2: The world should face the reality. *Environment International, 139*, Article 105730.

Muhammad, S., Long, X., & Salman, M. (2020). COVID-19 pandemic and environmental pollution: A blessing in disguise? *The Science of the Total Environment, 728*, Article 138820.

Mukherjee, A., & Agrawal, M. (2018). Air pollutant levels are 12 times higher than guidelines in Varanasi, India. Sources and transfer. *Environmental Chemistry Letters, 16*, 1009–1016.

Nair, M. M., Bherwani, H., Kumar, S., Gulia, S., Goyal, S. K., & Kumar, R. (2020). Assessment of contribution of agricultural residue burning on air quality of Delhi using remote sensing and modelling tools. *Atmospheric Environment, 230*, Article 117504.

Nakada, L. Y. K., & Urban, R. C. (2020). COVID-19 pandemic: Impacts on the air quality during the partial lockdown in São Paulo state, Brazil. *Science of The Total Environment, 730*, Article 139087.

NASA (2020a). *Aerosol optical depth.* (accessed 11 May 2020) https://earthobservatory.nasa.gov/global-maps/MODAL2_M_AER_OD.

NASA (2020b). *MODIS DATA - moderate resolution imaging spectroradiometer.* (accessed 11 May 2020) https://nsidc.org/data/modis/terra_aqua_differences.

OECD (2014). *The cost of air pollution: Health impacts of road transport.* OECD Publishinghttps://doi.org/10.1787/9789264210448-en.

Otmani, A., Benchrif, A., Tahri, M., Bounakhla, M., El Bouch, M., & Krombi, M. H. (2020). Impact of COVID-19 lockdown on PM_{10}, SO_2 and NO_2 concentrations in Salé City (Morocco). *The Science of the Total Environment, 735*, Article 139541.

Ottosen, T. B., & Kumar, P. (2019). Outlier detection and gap filling methodologies for low-cost air quality measurements. *Environmental Science Processes & Impacts, 21*, 701–713.

Pacione, M. (2006). Mumbai. *Cities, 23*, 229–238.

Paital, B. (2020). Nurture to nature via COVID-19, a self-regenerating environmental strategy of environment in global context. *The Science of the Total Environment, 729*, Article 139088.

PIB (2020). *Ministry of health and family welfare, update on novel coronavirus.* (accessed 8 May 2020) https://pib.gov.in/pressreleaseiframepage.aspx?prid = 1601095.

Police, S., Sahu, S. K., Tiwari, M., & Pandit, G. G. (2018). Chemical composition and source apportionment of $PM_{2.5}$ and $PM_{2.5-10}$ in Trombay (Mumbai, India), a coastal industrial area. *Particuology, 37*, 143–153.

R Core Team (2020). *A language and environment for statistical computing R Foundation for statistical computing.* Vienna, Austria (2020).

Saadat, S., Rawtani, D., & Hussain, C. M. (2020). Environmental perspective of COVID-19. *The Science of the Total Environment, 728*, Article 138870.

Saez, M., Tobias, A., Varga, D., & Barceló, M. A. (2020). Effectiveness of the measures to flatten the epidemic curve of COVID-19. The case of Spain. *The Science of the Total Environment, 727*, Article 138761.

Şahin, M. (2020). Impact of weather on COVID-19 pandemic in Turkey. *The Science of the Total Environment, 728*, Article 138810.

Sahu, S. K., & Kota, S. H. (2016). Significance of $PM_{2.5}$ air quality at the Indian capital. *Aerosol and Air Quality Research, 17*, 588–597.

Schiermeier, Q. (2020). Why pollution is plummeting in some cities - but not others. *Nature* News (9 April 2020). https://tinyurl.com/NatureNewsCOVID-19 (accessed 10 May 2020).

Scroll (2019). *Delhi is world's most polluted city; Kolkata, Mumbai also in top 10, says global air quality monitor.* (accessed on 14 May 2020) https://scroll.in/latest/943917/delhi-is-worlds-most-polluted-city-kolkata-mumbai-also-in-top-10-says-global-air-quality-monitor.

Setti, L., Passarini, F., De Gennaro, G., Baribieri, P., Perrone, M. G., Borelli, M., et al.

(2020). SARS-CoV-2 RNA found on particulate matter of Bergamo in Northern Italy: First preliminary evidence. *medRxiv*.
Sharma, A. K., & Balyan, P. (2020). Air pollution and COVID-19: Is the connect worth its weight? *Indian Journal of Public Health, 64*, 132–134.
Sharma, S. K., Mandal, T. K., Jain, S., Sharma, A., & Saxena, M. (2016). Source apportionment of $PM_{2.5}$ in Delhi, India using PMF model. *Bulletin of Environmental Contamination and Toxicology, 97*, 286–293.
Sharma, S., Zhang, M., Gao, J., Zhang, H., & Kota, S. H. (2020). Effect of restricted emissions during COVID-19 on air quality in India. *The Science of the Total Environment, 728*, Article 138878.
Shen, F., Zhang, L., Jiang, L., Tang, M., Gai, X., Chen, M., et al. (2020). Temporal variations of six ambient criteria air pollutants from 2015 to 2018, their spatial distributions, health risks and relationships with socioeconomic factors during 2018 in China. *Environment International, 137*, Article 105556.
Shi, X., & Brasseur, G. P. (2020). The response in air quality to the reduction of Chinese economic activities during the COVID-19 outbreak. *Geophysical Research Letters, 47* e2020GL088070.
Shrestha, A. M., Shrestha, U. B., Sharma, R., Bhattarai, S., Tran, H. N. T., & Rupakheti, M. (2020). Lockdown caused by COVID-19 pandemic reduces air pollution in cities worldwide. *EarthArXiv*. https://doi.org/10.31223/osf.io/edt4j.
Shukla, K., Kumar, P., Mann, G. S., & Khare, M. (2020). Mapping spatial distribution of particulate matter using Kriging and Inverse Distance Weighting at supersites of megacity Delhi. *Sustainable Cities and Society, 54*, Article 101997.
Sicard, P., De Marco, A., Agathokleous, E., Feng, Z., Xu, X., Paoletti, E., et al. (2020). Amplified ozone pollution in cities during the COVID-19 lockdown. *The Science of the Total Environment, 735*, Article 139542.
Srivastava, S., Kumar, A., Bauddh, K., Gautam, A. S., & Kumar, S. (2020). 21-day lockdown in India dramatically reduced air pollution indices in Lucknow and New Delhi, India. *Bulletin of Environmental Contamination and Toxicology,* 1–9. https://doi.org/10.1007/s00128-020-02895-w.
SSEC (2020a). *Terra orbit tracks.* (accessed 11 May 2020) https://www.ssec.wisc.edu/datacenter/terra/GLOBAL.html.
SSEC (2020b). *Aqua orbit tracks.* (accessed 11 May 2020) https://www.ssec.wisc.edu/datacenter/aqua/GLOBAL.html.
Tobías, A., Carnerero, C., Reche, C., Massagué, J., Via, M., Minguillón, M. C., et al. (2020). Changes in air quality during the lockdown in Barcelona (Spain) one month into the SARS-CoV-2 epidemic. *The Science of the Total Environment, 726*, Article 138540.
Tomar, A., & Gupta, N. (2020). Prediction for the spread of COVID-19 in India and effectiveness of preventive measures. *The Science of the Total Environment, 728*, Article 138762.
Venter, Z. S., Aunan, K., Chowdhury, S., & Lelieveld, J. (2020). COVID-19 lockdowns cause global air pollution declines with implications for public health risk. *medRxiv*. https://doi.org/10.1101/2020.04.10.20060673.
Wang, Y., & Chen, Y. (2019). Significant climate impact of highly hygroscopic atmospheric aerosols in Delhi, India. *Geophysical Research Letters, 46*, 5535–5545.
Wang, Q., & Su, M. (2020). A preliminary assessment of the impact of COVID-19 on environment – A case study of China. *The Science of the Total Environment, 728*, Article 138915.
Wang, P., Chen, K., Zhu, S., Wang, P., & Zhang, H. (2020). Severe air pollution events not avoided by reduced anthropogenic activities during COVID-19 outbreak. *Resources, Conservation, and Recycling, 158*, Article 104814.
Wang, Y., Yuan, Y., Wang, Q., Liu, C., Zhi, Q., & Cao, J. (2020). Changes in air quality related to the control of coronavirus in China: Implications for traffic and industrial emissions. *The Science of the Total Environment, 731*, Article 139133.
WHO (2016). *Global urban ambient air pollution database.* (accessed 9 May 2020) https://www.who.int/airpollution/data/who-aap-database-may2016.xlsx?ua = 1.
WHO (2020a). *WHO announces COVID-19 outbreak a pandemic.* (accessed 8 May 2020) http://www.euro.who.int/en/health-topics/health-emergencies/coronavirus-covid-19/news/news/2020/3/who-announces-covid-19-outbreak-a-pandemic.
WHO (2020b). *WHO coronavirus disease (COVID-19) dashboard.* (accessed 21 May 2020) https://covid19.who.int/.
WHO (2015). *Economic cost of the health impact of air pollution in Europe C le a n a i r, h e a l t h a n d w e a l t h.* (accessed 12 May 2020) http://www.euro.who.int/pubrequest.
Wu, J. T., Leung, K., Bushman, M., Kishore, N., Niehus, R., de Salazar, P. M., et al. (2020). Estimating clinical severity of COVID-19 from the transmission dynamics in Wuhan, China. *Nature Medicine, 26*, 506–510.
Wu, X., Nethery, R. C., Sabath, B. M., Braun, D., & Dominici, F. (2020). Exposure to air pollution and COVID-19 mortality in the United States: A nationwide cross-sectional study. *medRxiv* 2020.2004.2005.20054502.
Xie, Y., Dai, H., Dong, H., Hanaoka, T., & Masui, T. (2016). Economic impacts from $PM_{2.5}$ pollution-related health effects in China: A provincial-level analysis. *Environmental Science & Technology, 50*, 4836–4843.
Xie, Y., Dai, H., Zhang, Y., Wu, Y., Hanaoka, T., & Masui, T. (2019). Comparison of health and economic impacts of $PM_{2.5}$ and ozone pollution in China. *Environment International, 130*, Article 104881.
Yang, X., Yao, Z., Li, Z., & Fan, T. (2013). Heavy air pollution suppresses summer thunderstorms in central China. *Journal of Atmospheric and Solar-terrestrial Physics, 95*, 28–40.
Zambrano-Monserrate, M. A., Ruano, M. A., & Sanchez-Alcalde, L. (2020). Indirect effects of COVID-19 on the environment. *The Science of the Total Environment, 728*, Article 138813.
Zhao, X., Zhang, X., Xu, X., Xu, J., Meng, W., & Pu, W. (2009). Seasonal and diurnal variations of ambient $PM_{2.5}$ concentration in urban and rural environments in Beijing. *Atmospheric Environment, 43*, 2893–2900.
Zhu, Y., Xie, J., Huang, F., & Cao, L. (2020). Association between short-term exposure to air pollution and COVID-19 infection: Evidence from China. *Science of the Total Environment, 727*, 138704.